IEEE Access
Multidisciplinary ⋮ Rapid Review ⋮ Open Access Journal

Received January 27, 2022, accepted February 16, 2022, date of publication February 28, 2022, date of current version March 10, 2022.

Digital Object Identifier 10.1109/ACCESS.2022.3155460

Single- and Multi-Carrier Systems Affected by Impulsive Noise: Covid-19 View

NIKOLA ROŽIĆ[1], (Member, IEEE), PAOLO BANELLI[2], (Senior Member, IEEE), AND ANA MARUSIC[3]

[1]Department of Electronics and Computing, University of Split (FESB), 21000 Split, Croatia
[2]Department of Engineering, University of Perugia, 06125 Perugia, Italy
[3]Center for Evidence-Based Medicine, Department of Research in Biomedicine and Health, University of Split School of Medicine, 21000 Split, Croatia

Corresponding author: Nikola Rožić (nikola.rozic@fesb.hr)

This work was supported in part by the projects "Advanced Communications and Information Systems and Services" and "Research in Biomedicine and Health" at the University of Split, Croatia.

ABSTRACT In this work we present a fully stochastic model of performance analysis of single- and multi-carrier modulations (SCM and MCM) in communication systems affected by impulsive noise. The key performance of the model is the symbol error rate (SER), which is fully determined as a function of the system parameters, including the frame length, symbol power, white noise power, impulsive noise power, and the probability of the impulse events. We derive closed-form analytical expressions for the systems SER and compare them with simulation results, showing very good agreement for all the impulsive noise scenarios. Specifically, we show under which conditions a MCM system performs better than a SCM one, and vice versa, which can be used to apply an optimal switching policy that minimizes SER. The model developed for SCM and MCM systems is conceptually applied to the Covid-19 phenomenology and, consequently, the results obtained for SCM and MCM scenarios are interpreted to inform decision and management policies of social distancing (lock/roam). Specifically, we also show when the "roam" strategy performs better than the "lock" strategy, and vice versa, thus enabling the design of an optimal control policy that minimizes the mortality rate (MR). However, the proposed model for Covid-19, which assumes a similarity with SCM/MCM systems, may not be easy to be tested in practice in the absence of adequate statistical data. Therefore, any management decision should not be based (only) on the proposed model adapted to Covid-19, and necessarily requests the integration of experts opinions.

INDEX TERMS Single-carrier and multi-carrier systems, impulsive noise, symbol error rate, Gaussian mixture models, Covid-19 conceptual model, decision/management policy.

I. INTRODUCTION

Multicarrier modulations (MCM), and specifically orthogonal frequency-division multiplexing (OFDM) schemes, are widely employed in most of the wired and wireless communication systems. Theoretical analysis of the SER performance for MCM, is an interesting topic in communication systems. Indeed, although an exact closed-form expression for the output signal-to-noise ratio (SNR) of such OFDM systems is available for widely used impulsive noise models, the theoretical analysis of the associated symbol error rate (SER) has recently attracted many researchers due to the every increase of internet of things (IoT) applications.

The associate editor coordinating the review of this manuscript and approving it for publication was Kumaradevan Punithakumar.

There are a number of motivations for the widespread use of OFDM, i.e., multicarrier modulation [1], [2]. Among them, one is certainly the higher resistance of MCM to impulsive noise (ImpN) with respect to single-carrier modulations (SCM) [3], for realistic values of the ImpN and communication system parameters.

This work summarizes an unified Gaussian Mixture Model (GMM)-based analytical approach for SER analysis of OFDM systems affected by ImpN. In the first part, we develop the closed form expressions for the SER of SCM and MCM systems affected by impulsive noise represented by GMMs, including Bernoulli-Gaussian (BG), Middleton Class-A, as well as (approximated) alpha-stable noise. Actually, for mitigated systems, the residual distortion noise at the output of a non-linear suppressor should be modelled with a K-component GMM (K-GMM). However, mitigated systems

are widely investigated (see e.g. [4] and others), and they are not in the focus of this work, whose aim is also to show how the proposed analytical framework can be effectively used for Covid-19 outbreaks management.

When affected by ImpN, one of the important differences between MCM and SCM is that every noise impulse that shots an MCM signal in the time domain, does not affect just an information symbol, but all the symbols grouped in the MCM frame, which are coded in the frequency domain. The analysis presented in this work shows that a MCM system performs better than a SCM one, specifically when the impulse probability and the power are not too high. The theoretical SER performance has been compared with the results obtained by simulations, showing very good agreement for all realistic impulsive noise scenarios. Although the paper focuses on OFDM systems, the presented framework and conclusions can be easily extended to any other MCM system.

Recently, a number of stochastic models proved to be adequate in information and communication technology (ICT) disciplines (as well as in other scientific areas, such as economics, finance, etc.), have been found to be successful to also model virus infection events. For example, research on the propagation of computer viruses in communication networks featured by a very complex connectivity, have highly contributed to the understanding of Covid-19 spreading mechanisms [5]. On the other side, GMM has also received significant attention in modelling the typical ticktail temporary behaviour of Covid-19 (e.g., [6]).

The noticeable statistical similarities between a number of mechanisms in ICT and virology systems, encouraged researchers to speculate that they may be analysed by using the same mathematical frameworks. Herein we show how an accurate analysis of a specific communication system performance, can be similarly applied to analyze the performance of virus outbreaks management, and vice versa, as also stated in [7], [8]. This way, it is possible to highlight which decision/management policies can efficiently handle corona virus threats and, consequently, aid the society to cope with Covid-19 pandemic challenges, and specifically to keep the mortality rate (MR) as low as possible.

Specifically, to the best knowledge of the authors, this work is the very first attempt to apply the SER performance analysis of modern communications systems to the mortality rate (MR) ''performance'' analysis of Covid-19 epidemic.

The contribution of this work includes:

i) a generalized GMM-based unified approach for prediction of the SER performance in SCM and MCM (OFDM) communication systems, affected by arbitrarily distributed ImpN. In addition, the analysis is significantly extended by varying all the system parameters to obtain deeper insight in the differences of the SER performance for the two competitive SCM/MCM systems;

ii) a novel approach to model the Covid-19 phenomenology by adapting the fully stochastic analytical model developed in i);

iii) a proposal for Covid-19 decision/management policy designed according to a minimum mortality rate (MR) criterion.

The rest of the paper is organized as follows. Section II discusses related works in the literature and Section III briefly summarizes SCM/MCM system and noise models. Section IV presents the performance analysis approach, and Section V derives SER performance for frequency-flat non-fading OFDM system affected by K-GMM ImpN, where AWGN (1-GMM) and 2-GMM [3] are two particular cases. Numerical and simulation results for SCM/MCM are presented in Section VI. Section VII conceptually extends the analysis of SCM and MCM systems affected by ImpN to a Covid-19 scenario, focusing on the estimation of the MR based on the extended statistical model. Section VIII proposes detection method, and Section IX highlights the associated decision/management policies. Section X discusses some specific aspects of Covid-19 pandemic and identifies some possible research directions. Finally, some concluding remarks are drawn in Section XI.

II. RELATED WORKS AND STUDIES

A. RELATED WORKS FOR SCM/MCM SCENARIO

The output SNR and SER performance of uncoded and coded SCM and MCM, affected by impulsive noise, have been investigated in [3], [9] and [10]. Important results for coded MCM affected by Bernoulli-Gaussian (BG) and Middleton Class-A ImpN can be also found in [11], [12], whereas the effect of alpha-stable noise ImpN has been analysed in [12], [13], and specific results for power line communications (PLC) have been presented in [14]–[16]. Other fundamental results for the SNR/SER performance limits can be found in [17]–[19], where the authors derived the achievable pairwise error probability (PEP) bounds for OFDM systems affected by impulsive noise represented by a GMM.

Futhermore, performance analysis for MCM/OFDM systems equipped with impulsive noise suppressors, either for 4G cellular systems (UMTS-LTE), broadcasting (DVBT), local area networks (WiFi), or PLC, have been derived in [19]–[24]. Therein, sample-based non-linear suppressors simply clip, null, or both clip and null the complex envelope of the baseband received signal, when it overpasses (sub)optimal thresholds designed to maximize the output SNR. Recently, a significant attention has been given to some modified schemes targetting either internet of things applications, e.g., to support the narrowband IoT modes [25], or to new OFDM-based modulation techniques adapted to fit stringent low-power constraints [26].

B. RELATED WORKS AND STUDIES FOR COVID-19 SCENARIO

The well known susceptible-infectious-recovered (SIR) model [27]–[29] is a compartmental infection model, which assumes tracking of the number of individuals belonging to S, I, or R compartments. The collected data are plugged

into the set of ordinary differential equations that model the dynamic of the pandemic evolution, and possibly forecast its evolution, in order to estimate the model parameters, also in the presence of some control actions. Each member of the population typically progresses from susceptible (S) to the infectious (I), and at the end to the recovered (R) compartment. The original SIR model evolution is basically deterministic, although it can be extended to a statistical framework, such as in [5], [30], [31], and references therein.

Actually, there are many modifications and extensions of the SIR model that include births and deaths processes, where for instance, there is no immunity after recovery, i.e., the susceptible-infectious-recovered (SIS) model [28], or SIRS model [31], where recovery after immunity lasts only for a short period of time, or SEIS and SEIR models [32], where there is a latent period of the disease where the person is not infectious (E-Exposed), or the class M for maternally derived immunity is added, leading to the MSIR model where infants can be born with immunity. For instance, the authors in [32] analyse the management strategies of the epidemic course by using a susceptible-exposed-infectious-recovered (SEIR) epidemic model, which is defined by four first-order differential equations, whose parameters are estimated by real collected data. This way, the model is used to generate predictions and assess the effectiveness of the control measures (closures, mobility restrictions, social distancing), in a sustainability context. Authors in [33] focus on managing the virus infections by using artificial intelligence (AI) and deep learning (DL) methods, proposing an integrated approach to data sources, by means of an user-friendly platform for physicians and researchers.

For example, authors in [34] consider Covid-19 cases and mortality data from Feb. to Sept. 2020 and a deterministic SEIR compartmental framework to model possible trajectories of severely acute respiratory syndrome coronavirus 2 (SARS-CoV-2) infections to predict the course of the epidemic and to help planning an effective control strategy. Similarly, the authors in [35] propose a new model that considers eight stages of infection: susceptible (S), infected (I), diagnosed (D), ailing (A), recognized (R), threatened (T), healed (H) and extinct (E), termed SIDARTHE. The SIDARTHE dynamical model uses eight ordinary differential equations, describing the evolution of the population in each stage over the analysed time frame. In [36] the authors propose an integrated detection-estimation-forecasting framework based on tracking of the infection rate and detecting of the pandemic wave onset, to forecast the pandemic evolution as quickly as possible, assuming required reliability.

Recently, several studies such as [6] and [37], have demonstrated that a Gaussian distribution is quite effective to model the temporal evolution of the daily number of new cases (deaths, or alternatively infections) due to the COVID-19 pandemic disease, providing quantitatively correct descriptions for the monitored rates in many different countries during a single wave. Authors in [38] revisited the SIR model by fitting a GMM to the data in order to describe the differential rate of infections. Specifically, they computed the height, width, and position of the bell-shaped rate showing that the SIR is captured by the GMM within a finite range of time.

It is also interesting to note that, as discussed in [39], the virus power, therein called virus grip strength, can be considered as a powerful predictor of mortality, not only for elderly people but also for middle-aged and young people.

Today, the most popular statistical model for Covid-19 prediction is based on fitting the collected (prior) data, and it has been launched by the Institute for Health Metrics and Evaluation (IHME) [40]. Thus, the IHME model does not simulate the virus growth based on epidemiological assumptions and differential equations, but just by a least squares (LS) fitting of the available data on the mortality rate (MR) for a given geographic area. However, the IHME model, as any other model, is sensitive to a number of different social distancing measures, imposed by local and national government, such as school closures, non-essential business closures (including bars and restaurants), stay-at-home recommendations, and travel restrictions, and many other key variables that capture the time dynamics.

There are also some papers in other research areas such as ICT, economics, finance, etc., that propose alternative ways to recount threats and aid the society to cope with the Covid-19 fallbacks. For example, authors in [5], by modelling Internet as a free-scale network, studied the spreading of computer viruses in ICT networks exploating percolation theory arguments. Such stochastic epidemic models have been studied in different networks [6], [32], [38], and are recently applied to the COVID-19 pandemic [37]. Specifically, research on the propagation of viruses in computer networks characterized by a very complex connectivity have highly contributed to the understanding of the Covid-19 propagation mechanism.

III. SYSTEM AND NOISE MODELS

This section focuses on M-QAM single- and multi-carrier (OFDM) communications over frequency flat (nonfading) channels, affected by impulsive noise. Thus, we introduce in the following the associated system and noise models.

A. SYSTEM MODEL

Let's define $\mathbf{s}_q = \left[s_q[0], s_q[1], \cdots, s_q[L-1]\right]^T$ the qth information symbol to be transmitted on L orthogonal subcarriers of an OFDM system, as shown in Fig. 1. Assuming the data $\left\{s_q[l]\right\}_{l=0,\ldots,L-1}$ on different subcarriers are independent, with zero mean and same variance $\sigma_s^2 = E\left\{\left|s_q[l]\right|^2\right\}$, the time-domain OFDM symbol $\mathbf{x}_q = \left[x_q[0], x_q[1], \cdots, x_q[L-1]\right]^T$ is obtained by $\mathbf{x}_q = \mathbf{F}_L^H \mathbf{s}_q$, where $\mathbf{F}_L$ is the L-point unitary discrete Fourier transform (DFT) matrix [2], [41] and $(\cdot)^H$ is the Hermitian operator.

In the special case L=1, a multi-carrier modulated (MCM) system reduces to a single-carrier modulated (SCM) one.

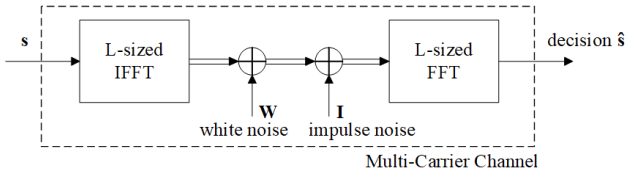

FIGURE 1. Conceptual scheme of the OFDM communication system.

B. IMPULSIVE NOISE MODELS

Generally, impulsive noise can be modeled by a K-GMM [42], whose probability density function (pdf) $f_N(n)$ is expressed by

$$f_N(n) = \sum_{k=0}^{K-1} p_k G(n, \sigma_k^2), \tag{1}$$

where $\{p_k\}_{k=0,1,\cdots,K-1}$, with $\sum_{k=0}^{K-1} p_k = 1$, are the probabilities that an impulsive event, with variance σ_k^2, is generated according to the kth Gaussian pdf $G(n, \sigma_k^2)$. The component $k = 0$ represents the "white" noise contribution, appearing with probability p_0 and variance σ_0^2, while the other $K-1$ components represent the impulsive noise, which appears with probability $p_I = \sum_{k=1}^{K-1} p_k = 1 - p_0$ and total variance $\sigma_I^2 = \sum_{k=1}^{K-1} p_k \sigma_k^2$.

The reason to choose model (1) are twofold. Firstly, K-GMM in (1) is a mixture of Gaussian functions, thus ensuring analytical tractability and elegance of calculation, and, secondly, K-GMM can successfully fit any ImpN distribution either exactly [43], [44], or approximately [45], [46].

Widely used ImpN models that are given by (1), include the well known Bernoulli-Gaussian (BG) and the Middleton's Class-A models. However, this approach can be obviously applied to any other noise that is modelled by a K-GMM including the symmetric alpha-stable (SαS) model [47], [48].

To make exposition easier, in this work we focus on the simple BG model [3], [19] which corresponds to a 2-GMM ImpN, where a noise sample is considered either thermal or impulsive, with probabilities p_0 and $p_1 = 1 - p_0$, respectively. The noise $W \sim G(w, \sigma_0^2)$ and the impulse noise $I \sim G(i, \sigma_1^2)$ are both zero-mean independent Gaussian RVs, resulting in ImpN with a total variance $\sigma_N^2 = p_0\sigma_0^2 + p_1\sigma_1^2$. The AWGN case is the even simpler case with $K = 1$ and $p_0 = 1$. However, for realistic systems, the K-GMM in (1) with $K > 2$ is generally important either as a very good approximation of the Class-A, SαS, or any nonGaussian ImpN distribution.

In this work, an ImpN is simulated by a K-GMM, which may represent an exact statistical distribution (e.g. BG, or Class A noise models), or an approximated one, such as for instance to model an alpha-stable ImpN, or any other actual process we may deal with. It is important to note that a K-GMM approximation of an ImpN with heavy-tailed distributions, such as the alpha-stable ones, can be well approximated only in a constrained amplitude range [47]–[49].

IV. PERFORMANCE OF SCM AND MCM AFFECTED BY ImpN

MCM are widely employed in most of the wired and wireless communication systems for several reasons. Among those, a reason is certainly their higher resistance to impulsive noise (ImpN) with respect to SCM [3]. As discussed in Sect. IIB, the BG model [3], [19] statistically describes the outcome of K=2 mutually exclusive events, which are interpreted either as "noise" or as an "impulsive noise".

As already stated, we will focus on 2-GMM, i.e., on the BG model, because it is both simple and sufficiently representative of an ImpN scenario. However, the results we show in this manuscript can be extended to any K-GMM with $K > 2$ leading to exact analytical expression for the SER of the communication systems impaired by K-GMM ImpN, thus generalizing the approach proposed in [3]. More detailed analysis based on the multinomial distribution [50] are also available in [4]. The simpler BG model is however enough to draw some general conclusions on the SCM/MCM adaptive policy to be adopted in a communication scenario and more importantly to highlight the potential usefulness of the some analytical framework to address Covid-19 restriction policies.

A. SER PREDICTION FOR 1-GMM (AWGN)

When $K = 1$, the well known SER formula for M-QAM square constellations in AWGN channels [1] is expressed by

$$p_s^{(AWGN)}(\rho) = 4\frac{\sqrt{M}-1}{\sqrt{M}} B_0(\rho)\left(1 - \frac{\sqrt{M}-1}{\sqrt{M}} B_0(\rho)\right), \tag{2}$$

where $B_0(\rho) = Q\left(\sqrt{\frac{3\rho}{M-1}}\right)$, and $\rho = \sigma_x^2/\sigma_n^2$ denotes the average SNR.

B. SER PREDICTION FOR 2-GMM ImpN

The two-component Bernoulli-Gaussian impulsive noise, as well as its distribution in the frequency domain after FFT demodulation, together with the associated SER, have been studied in [3]. Specifically, the pdf of the noise in the frequency domain, for an L-size OFDM frame, can be expressed by

$$f_N^{(f)}(n) = \sum_{l=0}^{L-1} w_l G\left(n, \sigma_l^2\right), \tag{3}$$

where w_l, $l = 0, 1, \cdots, L-1$ are the binomial scaling factors and σ_l^2, $l = 0, 1, \cdots, L-1$ are the noise variances given by

$$w_l = \binom{L}{l} p_1^l (1-p_1)^{L-l},$$
$$\sigma_l^2 = \left[(L-l)\sigma_0^2 + l\sigma_1^2\right]/L = [(L-l)\gamma_0 + l\gamma_1]\sigma_x^2/L, \tag{4}$$

and where p_1 and σ_1^2 are the impulse noise probability and the impulse noise variance, respectively, σ_0^2 is the variance of

the Gaussian noise component that appears with a probability $p_0 = 1 - p_1$, and $\gamma_0 = \sigma_0^2/\sigma_x^2$, $\gamma_1 = \sigma_1^2/\sigma_x^2$.

Given the SER $p_s^{(AWGN)}$ for AWGN in (2), the SER for 2-GMM impulsive noise can be expressed by

$$p_s^{(2-GMM)} = \sum_{l=0}^{L} w_l p_{s_l}^{(AWGN)} \tag{5}$$

where $p_{s_l}^{(AWGN)}$ is given by (2) with $B_l = Q\left(\sqrt{\frac{3\,\rho_l}{M-1}}\right)$, and $\rho_l = \sigma_x^2/\sigma_l^2 = L/(l_0\gamma_0 + l_1\gamma_1)$, with $l_0 = L - l$, $l_1 = l$.

Note that, under some circumstances, expression (5) can be used also as a good approximation for a K-GMM ImpN [20].

V. IMPULSE NOISE DETECTION PROBABILITY

The impulse noise detection problem in SCM/MCM communication systems is essentially a well known binary hypotheses test [51] where H_0: $y \sim p_{Y_0}(y)$ and H_1: $y \sim p_{Y_1}(y)$, and $p_{Y_0}(y) = p(y|H_0)$, $p_{Y_1}(y) = p(y|H_1)$ are the conditional probabilities. The associated maximum a posteriori (MAP) hypothesis test is expressed by the likelihood ratio

$$L(y) = \frac{p(y|H_0)}{p(y|H_1)} = \frac{p_{Y_0}(y)}{p_{Y_1}(y)} \underset{<}{\geq} \frac{p_1}{p_0}, \tag{6}$$

where $p_0 = p(H_0)$ and $p_1 = p(H_1)$ are the a priori probabilities.

The MAP test (6) assumes that the Bayes costs of erroneously decoding $\hat{H}_0$ for H_1, and vice versa, are the same, which however is not the case for the considered impulsive noise detection problem. This (sub)optimal detection threshold can be easily computed based on the intersection of the two weighted Rayleigh distributions as expressed by [24]

$$p_0 p(y|H_0) = p_1 p(y|H_1)\,. \tag{7}$$

Note that the best detection reliability would be obtained if the noise state information (NSI) is completely available, which however would correspond to a genie-aided detector (GAD) [52].

Thus, the threshold A_T can be obtained by the decision boundary condition, as expressed by

$$A_T = \arg_y \left\{p_0 p_{Y_0}(y) = p_1 p_{Y_1}(y)\right\}, \tag{8}$$

where $p_{Y_i}(y)$, $i = 0, 1$ are Rayleigh *pdf*s with variances $\sigma_{y_i}^2 = 2(1+\gamma_i)\sigma_x^2$, and characterize the received signal y under hypothesis H_i, leading to the closed-form expression

$$A_T = \sigma_x \sqrt{\frac{2(1+\gamma_0)(1+\gamma_1)}{\gamma_1 - \gamma_0} \log\left[\frac{p_0(1+\gamma_1)}{p_1(1+\gamma_0)}\right]}. \tag{9}$$

Given the suboptimal threshold A_T, the probabilities $P\{\hat{H}_0\}$ and $P\{\hat{H}_1\}$, to correctly decide for H_0 or H_1, are expressed by

$$\begin{aligned} P_{\hat{H}_0} &= \int_0^{A_T} p_{Y_0}(y)\,dy = \exp\left(-A_T^2/\sigma_{y_0}^2\right) \\ P_{\hat{H}_1} &= \int_{A_T}^{\infty} p_{Y_1}(y)\,dy = \exp\left(-A_T^2/\sigma_{y_1}^2\right), \end{aligned} \tag{10}$$

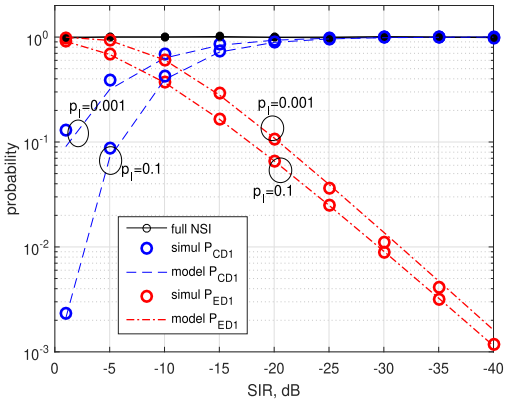

FIGURE 2. Comparison of the results for P_{CD_1} and P_{ED_1} obtained by (10) (denoted by "model") and by simulation.

where A_T is given by (9), and $\sigma_{y_0}^2 = 2\left(\sigma_x^2 + \sigma_0^2\right)$, $\sigma_{y_1}^2 = 2\left(\sigma_x^2 + \sigma_1^2\right)$.

Given the correct detection probabilities $P_{CD_0} = P\{\hat{H}_0|H_0\} = P_{\hat{H}_0}$ and $P_{CD_1} = P\{\hat{H}_1|H_1\} = P_{\hat{H}_1}$ in (10), the probabilities of erroneous detection P_{ED_0} and P_{ED_1} simply follow from $P_{ED_0} = 1 - P_{CD_0}$ and $P_{ED_1} = 1 - P_{CD_1}$.

Obviously, the reliability of the impulse noise detection directly depends on all the ImpN parameters. Fig. 2 compares the theoretical results for P_{CD_1} and P_{ED_1} obtained by (10) (denoted by "model") with those obtained by simulations. The results show that the probability of the impulse noise detection highly depends on the SIR and the probability p_I of an impulsive event. Specifically, the probability of correct detection of an impulsive event increases when either SIR or p_1 decreases, or both. Evidently, the detection can be considered quite reliable when SIR≤ -25dB.

VI. SER ANALYSIS

Numerical and simulation results presented in this section consider the SER performance of SCM/MCM with 4-QAM, varying the number of subcarriers from $L = 1$ (i.e., SCM) up to $L = 8192$, over nonfading channels affected by BG, or more generally a K-GMM ImpN. The SER performance are analyzed for a wide range of parameters of practical interest, including the SIR, the impulse probability p_I, as well as the "white" SNR defined by the signal-to-"white" noise power ratio $\sigma_x^2/\sigma_w^2 = 1/\gamma_0$.

Fig. 3 compares the SER performance for SCM ($L = 1$) and MCM from $L = 4$ up to $L = 8192$, for a 4-QAM OFDM system, at SNR=25dB and SIR$\in [-40, 0]$dB. The probability to be hit by an ImpN is $p_I = 0.001$. The results clearly show that, increasing the number L of subcarriers per MCM frame, noticeably improves the system performance for the highest SIR (i.e., SIR$\in [-20, 0]$dB), while conversely, the MCM system gets worse when SIR gets lower. Increasing L, it also widen the SIR range where MCM has better SER than SCM.

Fig. 4 shows the SER of both the SCM and MCM scenarios, for several values of SNR$\in$ [10, 30]dB, and SIR$\in$ [-60, 0]dB, and the impulse noise probability that is fixed

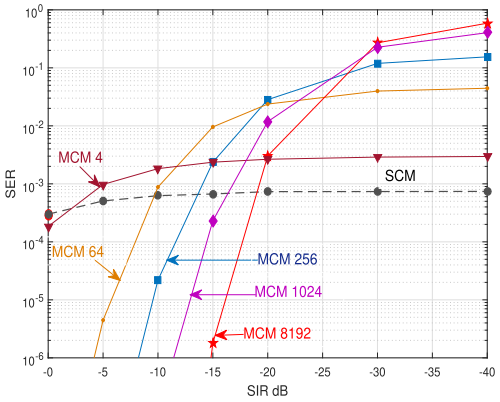

FIGURE 3. SER of SCM (L=1) and MCM when L∈[4, 8192], for 4-QAM communications, at SNR=25dB, and SIR∈[−40, 0]dB. The probability of ImpN is $p_I = 0.001$.

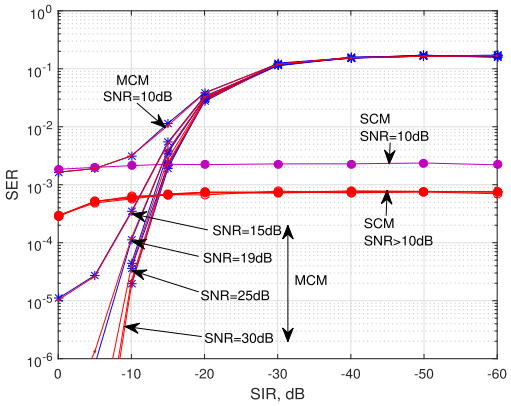

FIGURE 4. Comparison of SER performance for SCM (L=1)and MCM (L=256). The SNR parameter is considered in range 10 to 30 dB, and the SIR parameter vary from 0 to −60dB. The probability of ImpN is $p_I = 0.001$.

to a reasonable low value p_I =0.001. Evidently, Fig. 4 confirms that MCM schemes offer better SER performance with respect to SCM, at relatively higher SIRs (e.g., SIR ≥ -14dB), with a bigger performance gain for higher SNRs (e.g., almost 10 times lower SER at SIR = −10dB and SNR = 25dB). For relatively low SNRs (e.g., SNR $\leq$ 10dB), the performance gain of the MCM is negligibly low. On the contrary, for lower SIRs and higher SNRs, the SER performance of SCM is better than those of MCM schemes.

Fig. 5 compares the SER performance of SCM and MCM schemes, although at a different signal power expressed by S= σ_X^2. Actually, we compare the performance for a total signal power where S=1, and the performance for halved signal power where S=0.5, with SNR∈ [10, 30]dB, and SIR∈ [−40, 0]dB and the same impulse noise probability of Fig. 4, that is $p_I = 0.001$. As expected, the negative impact of a lower signal power is quite evident, since it decreases both SNR and the SIR, for fixed white noise power N and impulsive power I.

The SER performance, and the associated comparison for SCM and MCM, could be exploited in a cognitive communication system by designing an adaptive algorithm that optimizes the overall system performance by smartly

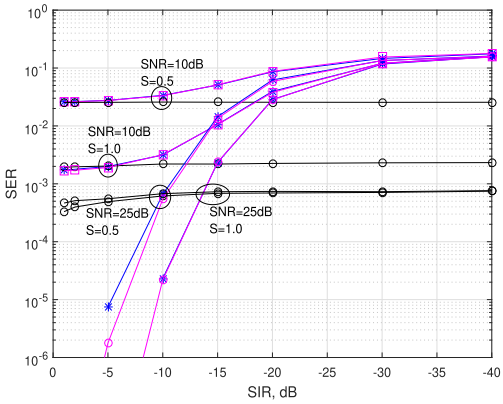

FIGURE 5. SER versus SIR for 4-QAM OFDM system with L=256 subcarriers affected by BG ImpN at $p_I = 0.001$ with SNR = 10 dB and 25 dB.

switching between MCM and SCM models, possibly taking into account not only the SER. Actually, it should be also reminded, that the SER performance can be significantly improved also by other approaches. First of all, the system may use very simple impulse noise mitigation techniques, and secondly, an error-correcting channel-code can be inserted to decrease the ultimate SER. Nevertheless, in practical communication systems, the analysis we proposed herein for uncoded SER performance, as detailed in the following sections, can be usefully exploited during Covid-19 outbreaks, in order to estimate the MR associated with two different restriction conditions (lock, roam), and possibly efficient control policies that minimize the ultimate MR, by switching among the two conditions.

VII. SCM/MCM MODEL APPLIED TO COVID-19 PHENOMENOLOGY

We essentially note that there is a phenomenological similarity of SCM/MCM systems affected by impulsive noise, and people affected by virus Covid-19. In this view, the SER performance of SCM/MCM systems affected by impulsive noise are conceptually related to the MR performance of the lock/roam policies for people living in an environment affected by the infective virus. Both cases are characterized by a pre-existing pathological condition, which is the erroneous decoding induced by AWGN for SCM/MCM and the typical mortality for the human population. Impulsive noises and Covid infections are further random events that worsen the pre-existing pathologies, thus increasing the errors and the mortality, respectively.

A. THE APPROACH

More specifically, we can distinguish the two following phenomenological conditions that highlight some similarities between the two different systems and their pathological states:

1) NO-IMPULSE NOISE/No-COVID VIRUS

In this case we can observe that:

i) the SER performance, without impulsive noise, depends only on the SNR and it is the same for SCM

and MCM systems. Consequently, it is not necessary to employ an SCM/MCM control to minimize the SER;

ii) the MR performance, without pandemic impact, depends only on the person immunity S and comorbidity C, i.e., we may assume it depends only on the person strength to comorbidity ratio (SCR) and, consequently, it is not necessary to employ any lock/roam control policy.

2) IMPULSIVE NOISE/INFECTIVE COVID VIRUS

In this case we observe that:

i) the SER performance of SCM and MCM systems, affected by impulsive noise, depends not only on the SNR, but also on the SIR and on the probability of the impulse p_I. This induces different SER in SCM and MCM, and, consequently, an SCM/MCM control is required to minimize the SER;

ii) the MR outcome, under pandemic impact, depends not only on the SCR, but also on the person strength S to the virus power I ratio, i.e, on the SIR, and on the virus attack probability p_I, which induce a different MR for ''lock'' and ''roam'' conditions and, consequently, a lock/roam control is required to minimize the MR.

Note that without the virus there is also a different MR, and the control policy is really simple: always ''roam''!. Furthermore, note that when the virus is absent, in contrast to SCM/MCM in AWGN, the ''roam'' policy is characterized by a lower mortality, as we will further motivate in the following.

Based on these similarities we observe that the ''performance'' of both systems are characterized by environmental random variables (RVs), which are the result of the superposition of two independent components. Specifically,

- in SCM/MCM systems, all the RVs that model the system condition are zero-mean complex-valued Gaussian-RVs with (equi-variance) independent real and imaginary components. Consequently, the magnitude is a Rayleigh distributed random variable.
- in the Covid-19 case, we assume that the random variables that model the person conditions are composed by two independent (additive) components, representing physical and psychological conditions. Here by simplicity we assume that also in this case the random variable representing the overall population strength could also be a Rayleigh distributed RV. However, this is not mandatory and the conceptual model and control policy can be adapted to any other *pdf* (see the following subsection).

We basically assume, that both the SER and the MR performance depend on the statistical distribution of the strength of the underlying quantities, i.e., they depend on the *pdf* parameters, or their moments, such as the power. A more detailed discussion on the conceptual equivalence of the *pdf* parameters in the two scenarios is addressed in the next subsection. In a nutshell, we claim that the analytical framework we highlighted for communication systems, can also be useful to define Covid-19 management policies, such as isolating (''lock'') people or letting them to freely move (''roam''). As we will motivate later, roaming or locking corresponds to preferring MCM rather than SCM in communication systems impaired by impulsive noise.

Based on this approach, Sect. X presents an adaptive (sub)optimal decision/management policy for Covid-19 pandemics with a goal to minimize MR.

B. COMPARISON OF SCM/MCM AND COVID-19 CONCEPTUAL MODELS

Let's compare the two conceptual models and, more specifically, the basic mechanisms of the communication system shown in Fig. 1, with those of the Covid-19 system shown in Fig. 6. It is important to note that the two models represent the main elements of a communication or a community social system, respectively. In the light of our assumption that the events observed in the two systems have similar phenomenology, associated to similar basic prevalence of one among two possible states, we foresee similar outcomes in terms of ultimate performance, that is SER and MR. We want anyway to stress that we overlook any virology or epidemiologic grounded consideration on the virus spread, and we simply observe the macroscopic final effects, leaving more specific analysis or micro-modelling on the subject to multidisciplinary domain-expert teams.

As discussed in subsection IIA, Fig. 1 presents the communication system model using SCM or MCM, which is affected by an additive white noise W and a superimposed impulsive noise I. Differently to W, which is a continuous Gaussian process, the impulsive noise has been modelled as a Bernoulli-Gaussian process, with a probability p_I to generate an impulsive event at any time epoch. Besides the channel, the two very important elements of the system in Fig. 1, are the IFFT and FFT blocks, which enable reliable MCM communications when a strong impulsive noise is present. Conversely, when the dominant noise is the AWGN one, we prefer SCM, where the processing cost associated with IFFT and FFT boxes is not necessary.

Similarly, Fig. 6 presents a model of a meeting social system that is possibly affected by some prior illness (comorbidity) of the people and by the superimposed spread of the infective Covid-19 virus. Similarly to SCM/MCM, the most important elements of the system in Fig. 6 are the grouping (gathering) and ungrouping (separating) blocks. The grouping box in Fig. 6, like an IFFT box in Fig. 1, defines a restricted group of L individuals that, due to the meeting environment, experience another socialization domain, which is different from the condition of lonely individuals, and has a positive impact on the underlying resistance to virus, when and if they will be exposed to it. Similarly to the FFT block, that in the communication model $\mathcal{A}$ spreads the white and impulse noises among all the symbols, the ungrouping box, spreads among the community the individual conditions, including both the comorbidity and the virus, as long as they are moderate. However, this negative effect, could

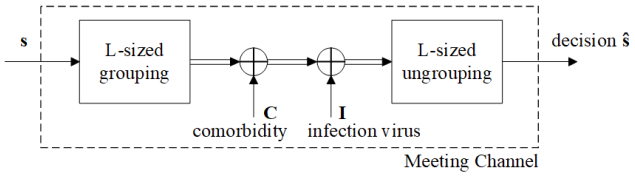

FIGURE 6. Conceptual scheme of the people meeting system (for Covid-19 scenario).

be compensated by the increased resistance associated with a higher socialization. Obviously, this spreading effect in Covid-19 scenario can be only conceptually considered as equivalent to the actual and physically grounded spreading effect of FFT in MCM case. The impulse noise and the viral spreading, are stochastic variables that strictly depend on the parameters and conditions that model the scenario of interest. While we almost perfectly know the actual physical model for communication systems, we assume herein that the overall effect caused by several simultaneous causes induces a similar stochastic effect in the Covid-19 meeting system, where the comorbidity plays the role of the background "noise" that induces the typical mortality, while the infection is a further detrimental effect to the average health conditions in the community, characterized by a random distribution.

The communications model $\mathcal{A}$ considers the symbol S as the result of a two-dimensional (i.e., complex-valued) modulation of the information signal. Similarly, in model $\mathcal{B}$, the individual strength S is assumed to be summarized by two independent components, which reflect both a physical and a psychological/social condition.

In model $\mathcal{A}$, the signal magnitude is denoted by S, and the associated signal power (variance) σ_S^2 by S, respectively. Similarly, in model $\mathcal{B}$, symbol S denotes the person strength (resilience), and S$=\sigma_S^2$ denotes the person power (immunity).

The symbol N denotes the total noise magnitude in model $\mathcal{A}$, with power σ_N^2 denoted by N. In model $\mathcal{B}$, we denote the person prior illness (caused by other acute and chronic diseases) magnitude by C, and its power (comorbidity) by C$=\sigma_C^2$.

Symbol I represents the impulsive noise magnitude in model $\mathcal{A}$, with power σ_I^2 denoted by I. Similarly, in model $\mathcal{B}$, symbol I represents the Covid-19 infective magnitude (strength), with power denoted by I$=\sigma_I^2$.

In this view, the parameters that we introduced so far can be re-interpreted as follows:

1) the SNR parameter, that represents the signal-to-noise power ratio in model $\mathcal{A}$, can be associated to the person power-to-comorbidity power ratio, which we address by SCR in model $\mathcal{B}$;
2) the SIR parameter, which defines the signal-to-impulse noise power ratio in model $\mathcal{A}$, can be interpreted as the person-to-virus power ratio, which we consequently denote as SIR also in model $\mathcal{B}$.
3) The probability p_I in model $\mathcal{A}$ corresponds to the probability that an impulsive source corrupts the signal in the channel, and p_I is the same for SCM and MCM scenarios. Similarly, in model $\mathcal{B}$, we denote by p_I the probability of an infective attack generated by a virus source to an individual, and we assume that p_I is the same for "lock" and "roam" scenarios, although this is not strictly necessary. Note however that the virus source in $\mathcal{B}$, just like the ImpN source in model $\mathcal{A}$, is something "outside" the communicating room (channel).

In light of the previous considerations, expression (5) obtained for model $\mathcal{A}$ can be reinterpreted for model $\mathcal{B}$. Obviously, for model $\mathcal{A}$, Eq. (5) computes the SER for MCM when $L > 1$, while it computes the SER for SCM when $L = 1$. Equivalently, when $L > 1$, Eq. (5) computes the MR for model $\mathcal{B}$ in "roam" scenario, as expressed by

$$\mathrm{MR} = p_s^{(\mathrm{roam})} = \sum_{l=0}^{L} w_l p_{s_l}^{(\mathrm{AWGN})}(\rho_l), \tag{11}$$

where $p_{s_l}^{(\mathrm{AWGN})}(\rho_l)$, w_l and ρ_l are given by (2), (4) and (5), respectively.

Having in mind that the person strength S consists of two independent components, due to the equivalence of models $\mathcal{A}$ and $\mathcal{B}$, we can use $M = 4$ in (5), leading to $B_0(\rho) = Q\left(\sqrt{\rho}\right)$, and the average SCR ρ is expressed by $\rho = \frac{\mathrm{S}}{w_0\gamma_0 + w_1\gamma_1}$, with $w_0 = 1 - w_1$, $w_1 = p_I$, and $\gamma_0 = \mathrm{C/S}$, $\gamma_1 = \mathrm{I/S}$.

Similarly, the MR expression for the "lock" scenario where $L = 1$, is expressed by

$$\mathrm{MR} = p_s^{(\mathrm{lock})} = w_0 p_{s_l}^{(\mathrm{AWGN})}(\rho_0) + w_1 p_{s_l}^{(\mathrm{AWGN})}(\rho_1). \tag{12}$$

1) ADDITIONAL NOTES

i) In our approach, we assume that the individual age impacts the comorbidity C, rather than the immunity I. Thus, we assume that the immunity does not depend on the age, but on the life conditions, harmony in the family, working environment, friendly human communications, social and business success, i.e., to the all that can significantly affect the individual resilience, that is the immunity.
ii) the probability p_I in model $\mathcal{B}$ should not be considered as the probability of infection, which is typically tracked in practice [53]. Namely, the roaming model considered in this work, assumes free meetings and free communications between people, and all group members are expected to be, on average, infected at the same level (as it happens in MCM systems with impulsive noise spreading by FFT processing). Thus, p_I in our framework is just the probability of an infective attack, generated by a virus source.
iii) the frame size L in model $\mathcal{A}$ is considered as the fixed value for which the SER performance is investigated. However, L can vary as a function of time to fit different service parameters or environmental conditions. Thus, L could be generally considered as a random variable on a long run, and, consequently, the total SER should

be computed as the weighted average for the given distribution of L. In model $\mathcal{B}$, the size L naturally varies from a roaming condition to another, and consequently the total MR should be computed as the weighted average for the given distribution of L.

iv) in model $\mathcal{A}$, the semi-positive magnitudes $|X|$, $|W|$ and $|I|$ are Rayleigh distributed, reflecting the high number of micro-events that could possibly determine the channel behaviour. This fact, by Central Limit Theorem arguments induces a Gaussian distribution of the (complex) random variables that describe the system. Similarly, we assume that the magnitudes (strengths) S, C and I in model $\mathcal{B}$ are also Rayleigh distributed reflecting the high complexity of all the possible events in the human infection by Covid-19 scenario. Unfortunately, an analysis of the statistical distribution of the Covid-19 infective strength that we postulate in this manuscript, is not available in the literature. Note however that, although we assume a Rayleigh distribution for simplicity, this fact does not affect the overall conceptual approach: actually, by observing that the distribution of any semi-positive RV can be approximated by a Rayleigh scaled mixture model K-RMM [54], [55]. Similarly to the approximation by K-GMM of any double-sided RV, it is possible to extend the results we show herein to any other distribution, similarly to what it has been done for MCM systems [4], [56].

C. RELATION OF COVID-19 AND SCM/MCM CONTROL PROTOCOLS

An individual who is isolated and lives ''alone'', or simply ''locked'', should not meet and communicate ''face to face'' with other people including his family, colleagues and friends, while he might communicate at most virtually (i.e., on-line). Thus, the locked individual will experience a reduction in almost all beneficial effects induced by socialization. However, this individual is not free of the infective attacks from the virus source(s). Indeed, such ''isolated'' individual is sometimes exposed to short meetings with someone that is really close to him, such as a familiar, or any other person who is visiting him. Thus, this individual is also actually exposed to spreading of Covid-19, although at a lower extent. Such, ''locked'' individuals, in our parallelism, may be conceptually associated to the ''information symbols'' in model $\mathcal{A}$ that are separately transmitted through the communication channel, and are exposed to infection by Covid-19 virus, with a probability p_I. Thus, this scenario resembles the SCM system, where just a single information symbol is impaired by an impulsive event. Therefore, for isolated, i.e., ''locked'' individuals, we can apply SER performance results in model $\mathcal{A}$ for the SCM scenario, which in the Covid-19 scenario has to be interpreted as the probability of an extremely serious infection, or to make it simpler, as a proxy of the ''mortality rate'' (MR). Let's also establish that an isolated (locked) individual would experience a decrease of his power and will feel noticeably worse than when the individual was free to move and meet other people, with a consequent decrease of the immunity. Such assumptions are widely confirmed by doctors and psychologists [57].

Conversely, a person who freely ''roams'', has more opportunities to meet and communicate face-to-face either walking along the promenade, visiting shopping centers, or being with friends, in restaurants and coffee bars, etc. Thus, a ''roaming'' person is factually exposed to contacts with very different individuals and, being in face-to-face communication with more or less large groups (similarly to the frame of information symbols transmitted through the MCM communication channel), can be attacked by probability p_I, and infected by the Covid-19 virus with a certain infective power. People meeting other people, share experiences, and the infection as well. This scenario in model $\mathcal{B}$, can be conceptually related to a MCM system where all the symbols in a frame are mixed by the IDFT processing at the transmitter and then sent through the channel. Therefore, for ''roaming'' persons, the MR can be related with the SER performance of model $\mathcal{A}$ with an MCM scenario. It is also important to note that a ''roaming'' person while meeting other people also improves their body and spirit, and experience friendship through sharing their mental power. Persons clearly feel increasing of the power and feel noticeably better, thus increasing their strength, i.e., the immunity.

Understandably, it is not likely that our qualitative analysis of the ''roaming'' scenario could be tested in experimental conditions, differently from the use of MCM in model $\mathcal{A}$, which can be actually tested in practice. However, the presented phenomenology helps us to understand why model $\mathcal{B}$ may be considered as conceptually equivalent to model $\mathcal{A}$.

D. REINTERPRETATION OF THE PERFORMANCE RESULTS FOR SCM/MCM TO COVID-19 SCENARIO

In this subsection, we illustrate the MR performance results which actually reflect the conceptual duality between model $\mathcal{A}$ for SCM/MCM scenarios, and model $\mathcal{B}$ for Covid-19 lock/roam scenarios. Additional notes on the parameters that control the MR results are given in Sect. X.

Fig. 7 reinterprets Fig. 3 and shows the MR for ''lock'' ($L = 1$) and ''roam'' scenarios ($L = 4$ to $L = 8192$) for model $\mathcal{B}$, at SCR=25dB and SIR from 0 to -40dB. The probability of virus attack is $p_I = 0.001$. The results clearly show that, for higher SIR and L, increasing the number of people in a meeting, noticeably improves the MR performance and conversely, for low SIR, the MR performance of the ''roam'' scenario gets worse with increasing L. This fact simply confirms, as expected, that locking people in the absence of a strong pandemic scenario worsens the MR due to the pandemic detrimental effect of being alone, especially for elderly people, exactly as it happens in the absence of the pandemic.

Fig. 8 reinterprets Fig. 4 and illustrates the MR, comparing it for ''lock'' and ''roam'' scenarios. The parameter SCR is considered in the range [10,30] dB, while the person

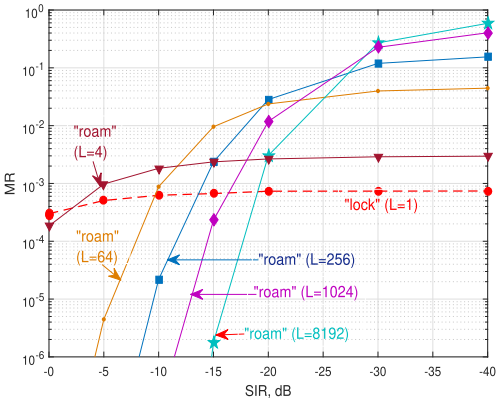

FIGURE 7. Comparison of MR performance for "lock" (L=1) and "roam" (L=4 to L=8192) scenarios, at SCR=25dB, and SIR∈[0,−40]dB. The probability of the infective virus attack is $p_I = 0.001$.

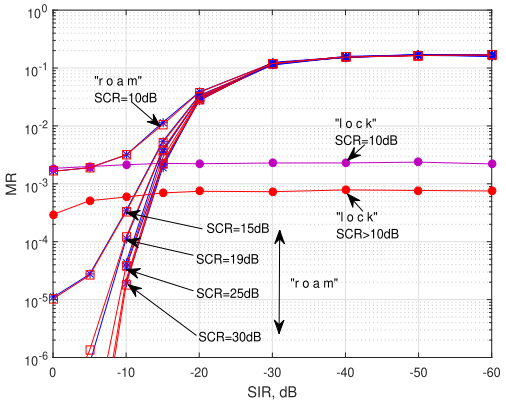

FIGURE 8. Comparison of MR for "lock" and "roam" scenarios. The SCR parameter range is 10 to 30 dB, and the SIR∈[0:60]dB. The probability of infective attack is $p_I = 0.001$. "Roam" results are obtained for L=256.

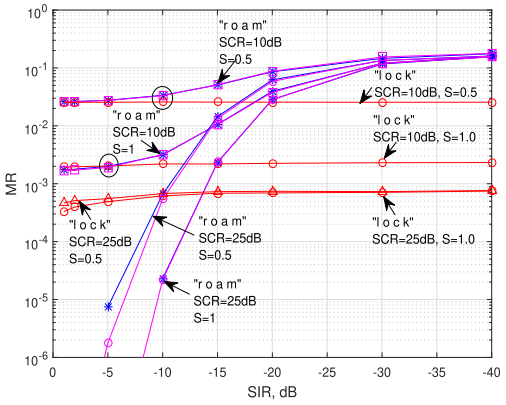

FIGURE 9. MR comparison for "lock" and "roam" scenarios for immunity S=0.5 and S=1.0, and SCR∈[10:30] dB, SIR∈[0:40] dB. The probability of the infective attack is $p_I = 0.001$. "Roam" results are obtained at L=256.

power-to-Covid infective power ratio SIR∈[−60,0]dB. The probability of the virus attack is $p_I = 0.001$. Equivalently to the comments provided for Fig. 4, it is evident that the "roam" scenario offers better performance than the "lock" scenario, for higher SCRs and higher SIRs (e.g., SIR≥ −14dB), with a performance gain that is higher for higher SCRs (e.g., about 10 times higher for SIR= −10dB and SCR = 25dB). For relatively low SCRs (e.g., SCR ≤ 10dB), which reflect a high comorbidity, the performance gain of the "roam" scenario is negligible. On the contrary, for lower SIRs, the "lock" scenario performs better than the "roam" scenario.

Fig. 9 actually reinterprets Fig. 5, and compares the MR performance for the "lock" and "roam" scenarios, as a function of the different person immunity. Actually, we compare the MR of persons at a full immunity characterized by S=1, with the MR for persons with medium immunity associated with S=0.5. The person strength-to-comorbidity ratio (SCR) is considered in the range [10,30] dB, and the person-strength to Covid-19 infective power ratio (SIR) varies in [−40,0] dB. The probability of an infective event is the same as in Fig. 5, i.e., $p_I = 0.001$. The impact of the decline in immunity is quite evident, which however is expected, since the lower S directly decreases both SCR and SIR for a given comorbidity C and a given virus power I. Specifically, the results in Fig. 9 show that the decline in immunity from S=1 to S=0.5 results in a noticeable increase of MR in both (lock and roam) scenarios. The impact of the comorbidity (i.e., SCR) is lower, and only highly healthy (SCR=25dB), but locked, individuals, do not experience serious increase of the MR. This somewhat unexpected result is however a consequence of the fact that a halved S induces a 3dB decrease of the SCR, leading to SCR=25-3=22dB, which does not noticeably increase the MR in locked case.

Differently from Fig. 9, Fig. 10 compares "lock" and "roam" scenarios for different values of the person strength (immunity). As discussed in the previous subsection, a locked person clearly experiences a decrease of strength and feels noticeably worse, thus resulting in a decrease of immunity. On the contrary, roaming persons feel noticeably better, with a consequent increase of actual immunity. Thus, Fig. 10 compares "lock" and "roam" strategies where we assumed that in the "lock" case the immunity S is halved (i.e., SCR=0.5) with respect to the "roam" scenario, where we used S=1. Comparing the analytical results with those in Fig. 9, we note an additional significant benefit for the "roam" scenario, especially at low SCRs. For example, when SCR=10dB, the immunity is S=1 for "roam" individuals and S=0.5 for "lock" individuals, the roaming scenario shows significant gain (i.e., 10 fold greater MR reduction or more), with respect to the locked one. In practice, we may assume that a low SCR (e.g., 10 dB) is more probably related with elderly people and, consequently, locking them leads to a higher MR. Thus, in order to minimize MR, we may be tempted to conclude that people with high comorbidity, i.e., with low SCR, who are locked, and consequently loose the natural immunity relatively fast, should probably be simply unlocked, letting them to freely move around ("roam" scenario), meet friends, colleagues etc., such that they can reach a full self resistance "immunity" of S=1.

It is important to note that, due to the assumed Rayleigh distribution, an immunity-to-Covid-19 infective

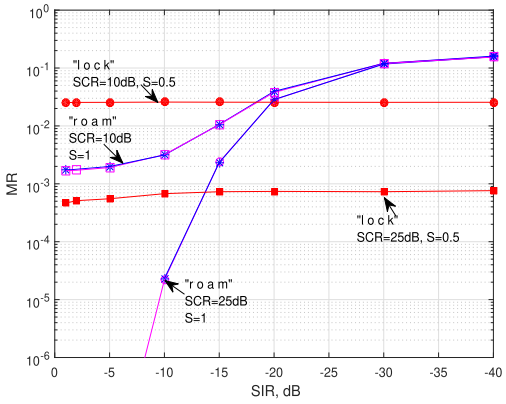

FIGURE 10. The immunity impact to MR for S=0.5 and S=1.0, at SCR=10 and 25 dB for "lock" and "roam" scenarios. The probability of the virus attack is $p_I = 0.001$. "Roam" results are obtained at L=256.

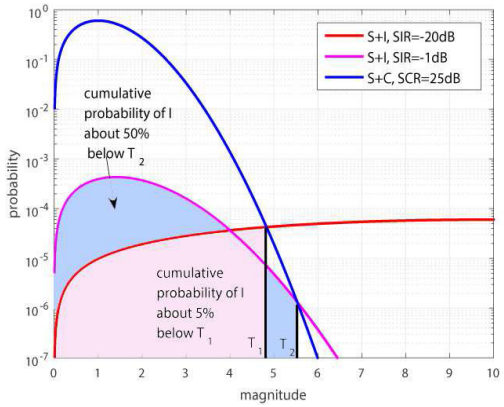

FIGURE 11. Rayleigh distributions for $S+C$ (blue) and $S+I$ (red/magenta), and the optimal threshold-based detecting probability for two typical scenarios: 1) SIR= −1dB and 2) SIR= −20dB, at SCR= 25dB and $p_I = 0.001$.

power ratio (SIR) of −10dB (i.e., the power of Covid-19 infection is ten times higher of the person power), doesn't necessarily mean a very dangerous situation for an individual. This can be explained by the following: i) the actual strength of an infective single event is defined by the Rayleigh distribution, and ii) the power of an infective event, in the roaming scenario, is spread over all the persons in the considered group. The spread effect is basically caused by spontaneously avoiding the continuous facing with the virus carrier(s), due to the opportunity to communicate with a number of people meeting them in walking, moving around or participating in other social activities.

VIII. DETECTION PROBABILITY OF INFECTION

As discussed in Sect. V, the key element of noise impulse detection techniques employed in SCM/MCM systems is the (sub)optimal threshold, which enables to decide whether the system is either in state H_0 (no impulse) or state H_1 (impulse), as a classical binary hypothesis testing (HT). The threshold can be easily computed from (9) and the reliability of the detection directly depends on the environmental parameters such as SNR and SIR.

A similar HT can be formulated on the specific strength, comorbidity and lock-roam condition and for Covid-19, to decide whether a person is in state H_0 (not infected) or in state H_1 (infected) according to a detection threshold that can be computed as in (9), under the assumption we made herein, or by similar equations for other statistical distributions of the person strength, comorbidity and virus infectivity. The decision, and its reliability, directly depends on the SCR and the SIR parameters. A certain detection unreliability is induced by the highly similar symptoms of Covid-19 with other diseases included in the comorbidity, which may induce similar values of any strangth indicator we want to use to asses the health condition of an individual, just as it may happen to confuse white noise with impulse noise in SCM/MCM. In a nutshell, a number of comorbidity symptoms may mask those for Covid-19, with a higher probability as the virus power goes lower. For example, Covid-19 and influenza viruses have a similar disease onset, since they both cause respiratory problems, characterized by a wide range of severity, spanning from asymptomatic to mild and severe symptoms, and possibly death. The noticeable difference between the two viruses is the transmission speed. Actually, influenza has a shorter median incubation period (the time from infection to appearance of symptoms) and a shorter serial interval (the time between successive cases) than Covid-19 virus, while Covid-19 is more infective [58], [59].

Consequently, in Covid-19, infection testing is regularly used to detect the positivity/negativity to Covid-19 virus infection of an individual, which can be modeled equivalently to the SCM/MCM case. Therefore, the (sub)optimal detection threshold can be computed based on the intersection of the weighted Rayleigh distributions for any given population average SIR and SCR, as illustrated in Fig. 11 which shows the Rayleigh distributions of $S + C$, and $S + I$ for two typical scenarios: 1) SIR $= -1$dB and 2) SIR $= -20$dB; at SCR $= 25$dB and $p_I = 0.001$ with depicted (sub)optimal detecting thresholds T_1 and T_2. The probability of the wrong detection of positivity to Covid-19 diagnosis can be calculated as the cumulative probability of I to be below the threshold T (coloured areas). Let $\underline{P_T}$ denote the cumulative probability of I to be below the threshold T. As shown in the figure for the two examples of SIR $= -1$dB and SIR $= -20$dB, the cumulative probability $\underline{P_T}$ for SIR $= -1$dB is about 0.5, and $\underline{P_T}$ for SIR $= -20$dB is about 0.05, respectively. It is reasonable to assume that the missed detection cases are directly related with the asymptomatic, but factually positive individuals. It is interesting to notice that, for any fixed threshold T, a higher probability $\underline{P_T}$ obviously corresponds to a lower virus power I (i.e., higher SIR), and vice versa. Consequently, a higher $\underline{P_T}$ (higher SIR), obviously leads to a lower MR. Thus, the roaming scenario should be preferred, when a high value of $\underline{P_T}$ is estimated by the model.

It can be seen from the figure that it is easy to compute the percentage of infected and symptomatic persons, as well as of

the infected but asymptomatic ones, for any set of the parameters, including SIR, SCR and p_I. Referring to Fig. 11, it is evident that there is a relatively high percentage of infected but asymptomatic persons when the infection power is low, i.e., when the SIR is close or greater than 0 dB. Consequently, as shown in Fig. 10, when SIR is close to 0dB, the better strategy is to leave people freely move around (''roam'').

A. IMPACT OF THE COMORBIDITY TO COVID-19 INFECTION

Similarly to possible impulse noise event in model $\mathcal{A}$, an infective attack in model $\mathcal{B}$ should not necessarily produce a pathological effect to an individual, but it could be, by a certain probability, more or less compensated by some individual's comorbidity component(s). This compensating effect will appear more probably for individuals with high comorbidity (typically elderly persons). Naturally, the overall effect of the coronavirus infection is more or less harmful, and the potential benefit of the mentioned compensation is in the reduced probability that each virus attack will result in an infection.

1) MODEL $\mathcal{A}$ CASE

In model $\mathcal{A}$, the compensation (masking) effect appears in every case when the amplitude of both the impulse noise components (real, imag) are more or less below the amplitude of the corresponding white noise components. Consequently, the magnitude $|W + I|$ is below the magnitude $|W|$, when the W and I components have opposite sign. The masking probability $P_m = P\{|W + I| \leq |W|\}$ of such ''impulse noise suppressing'' events can be computed by

$$P_m = \int_0^\infty f_{|W|}(w) \int_0^w f_{|W+I||W|}(n; |w|)\mathrm{d}n\mathrm{d}w. \quad (13)$$

Given $|W|$ and $|W + I|$ Rayleigh distributed, and assuming that the conditional pdf $\{p(|W + I|)\}|_{\{|W+I|\leq|W|\}}$ can be approximatively considered also Rayleigh distributed, expression (13) becomes

$$P_m \cong \int_0^\infty \frac{w}{\sigma_W^2} \mathrm{e}^{\frac{-w^2}{2\sigma_W^2}} \int_0^w \frac{n}{\sigma_W^2 + \sigma_I^2} \mathrm{e}^{\frac{-n^2}{2(\sigma_W^2+\sigma_I^2)}} \mathrm{d}n\mathrm{d}w, \quad (14)$$

which admits the closed form solution

$$P_m = \frac{\sigma_W^2}{\sigma_I^2 + 2\sigma_W^2}. \quad (15)$$

Following (15), the maximum healing probability equals 0.5, which is obtained at the limit when σ_I^2 approaches zero, i.e., SIR is very high (e.g., 30 dB), however, the case $\sigma_I^2 = 0$ means that there isn't any impulse and the compensation benefit disappears. When $\sigma_I^2 = \sigma_W^2 = 0.5$ (i.e., SNR=SIR=3dB) the probability P_m obtained by (15) is about 0.3.

2) MODEL $\mathcal{B}$ CASE

Fig. 12 reinterprets (15) for the coronavirus model $\mathcal{B}$ and plots the probability P_m when SCR spans from 0dB to 30dB, and for SIR values in {20, 3, −3, −10, −20} dB. Obviously, when the SCR is increases (i.e., the comorbidity is decreases) the probability P_m is decreasing, and vice versa. For a fixed SCR, an increase of the SIR (i.e., a decrease of the virus power) induces an increase of the P_m, and vice versa.

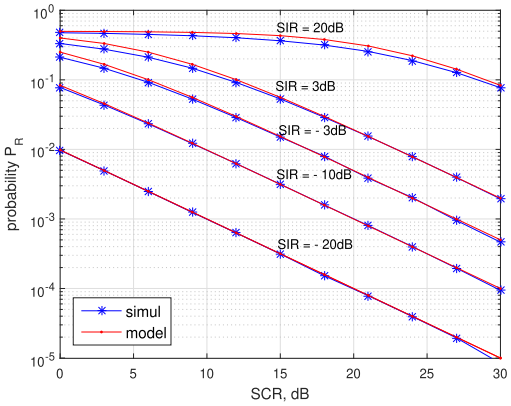

FIGURE 12. Probability of "masking" effect obtained by (15) for SCR spanning from 0dB to 30dB, and for SIR={20, 10, 0, −10, −20, −30}dB. Slight discrepancy of the model (15) results and the simulation results is due to Rayleigh approximation of the conditional density p(|W+I|).

Thus, assuming the statistical model developed for model $\mathcal{A}$, in the Covid-19 case (model $\mathcal{B}$) the compensation effect could appear any time the infective attack does not overpass the comorbidity, and the infective event appears to be more or less reduced by the individual's comorbidity. Simultaneously, although it may seem a bit surprising, the potential infective event appears to be a ''healing'' event to the pre-existing comorbidity, which an individual who avoids Covid-19 and may probably even feel better. Experts in the virology area explain this effect by the impact of the influence of viral antibodies in individuals with high comorbidity [60]. This ''healing'' effect is important for an individual who hopefully will not be exposed to infective events in a future, thus a ''lucky person'' will be more or less healthier, due to ''lucky'' meeting with a coronavirus. It could be said that a person burdened by another disease, through the infective event, may receive in some cases a sort of ''medical treatment'' for some of their comorbidities.

IX. DECISION/MANAGEMENT SYSTEM PROPOSAL

Assuming the knowledge, or estimate, of the virus power $\mathrm{I} = \sigma_I^2$, the virus probability p_I, the person power $\mathrm{S} = \sigma_S^2$ and the comorbidity power $\mathrm{C} = \sigma_C^2$, the results on the predicted MR can be obtained by expression (11) for the scenario with $L > 1$ by $\mathrm{MR} = p_s^{(\mathrm{roam})}$, or by expression (12) when $L = 1$ by setting $\mathrm{MR} = p_s^{(\mathrm{lock})}$. In order to minimize the MR, it can be concluded that, given $p_s^{(\mathrm{lock})}$ and $p_s^{(\mathrm{roam})}$, the control policy for model $\mathcal{B}$ should work as follows:

- if $p_s^{(\mathrm{lock})} \geq p_s^{(\mathrm{roam})}$ decide for the ''roam'' scenario
- if $p_s^{(\mathrm{lock})} < p_s^{(\mathrm{roam})}$ decide for the ''lock'' scenario

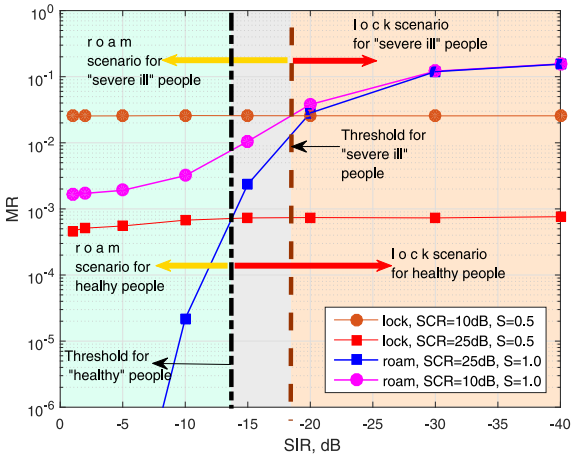

FIGURE 13. Decision/management Covid-19 chart: two almost limit cases, including the "severely ill" and the "healthy" subpopulations are described by two thresholds each, denoting the "lock" (right side) and "roam" (left side) decisions. The virus attack probability is $p_I = 0.001$.

Given S, C and p_I, the MR depends on the virus power I. If $\gamma_T = 1/\text{SIR}_T$ denotes the inverse value of the SIR_T, that identifies the decision threshold, and is calculated by

$$\text{SIR}_T = \arg\{p_s^{(\text{lock})} = p_s^{(\text{roam})}\}, \tag{16}$$

where $p_s^{(\text{roam})}$ and $p_s^{(\text{lock})}$ are expressed by (11) and (12), respectively.

Following the concluding remarks on the benefit of MCM compared to SCM, and vice versa, we note that for Covid-19 the "roam" scenario is characterized by a lower MR than the "lock" scenario when either the virus power or the virus probability, are not too high. On the contrary, when the virus power I and the virus probability p_I are both relatively high, the "lock" scenario performs better than the "roam" scenario, i.e. providing the lower MR among the two.

Based on these results, a (sub)optimal decision/management policy for Covid-19, supported on the criterion of the minimal MR, is proposed. Since all the parameters, including S, C, I, and p_I can vary by time, countries, regions, institutions, etc., the proposed decision/management system can easily adapt to each specific population category.

Fig. 13 interprets the results already shown in Fig. 10 in the light of the Covid-19 management policy we propose, where we highlighted the the decision thresholds computed by (16), for different values of the population SCR parameter.

Specifically, Fig. 13 shows that for very "healthy" persons characterized by SCR = 25dB, even a significant lower immunity of S = 0.5 does not noticeably increase the MR. However, for "severely ill" persons, such as many elderly people that are characterized by a high comorbidity (SCR=10dB), a lower immunity of S=0.5 significantly increases the MR.

The results we show in Fig. 9 and13 are inspired by a vision that, for "severely ill" persons is reasonable to assume that the lock (isolation) scenario could induce a lower personal strength (immunity), such as S=0.5, while the roaming scenario may favour a maximal natural immunity, such as S=1. This could be simply motivated by the fact that the severely ill persons, and particularly elderly ones, are highly sensitive to absence or presence of "the human touch". Naturally, this doesn't mean that the severely ill persons immunity switches immediately from, e.g., S=1.0 to S=0.5, or vice versa, although in reality it happens in a relatively short transient time.

By this perspective, Fig. 13 shows two borderline decision thresholds, both computed by (16), where one is for the "healthy", and the other one is for the "severely ill" population, respectively. The relatively wide gap between them (greyish part) highlights the SIR value where the control policy for the minimum MR depends on the actual parameters S and C (actually the SCR) for the considered population. It is interesting to note that, differently from the generally accepted opinion, the decision threshold related to the population with high comorbidity, suggests the "roam" scenario even when the virus power I is relatively high (i.e., with arelatively low SIR), while the corresponding decision for "healthy" population would be evidently "lock". This somewhat unexpected result is, however, a consequence of the sensitivity of the elderly persons immunity to isolation.

As also shown in Fig. 13, for the "lock" case and relatively healthy people (SCR=25dB), given a probability of virus attacks of $p_I = 0.001$, the mortality rate is about $0.75p_I$ and it is almost independent of the virus power, i.e., the SIR. Obviously, the policy based on the minimization of the MR suggests that the locked scenario should be switched to the roaming scenario if SIR ≥ -13dB.

For people with relatively low person power-to-comorbidity ratio, such as SCR = 10dB, the mortality rate is about $25 \cdot 10^{-3}$ in the locked scenario, almost independently of the SIR. However, for the roaming scenario and SIR ≥ -18dB, the minimization of the MR suggests to switch from the locked to the roaming scenario, in order to significantly reduce the MR, e.g. MR$= 2.5 \cdot 10^{-3}$ at SIR $= -10$dB, and MR$= 1.5 \cdot 10^{-3}$ at SIR $= 0$dB.

It should be noticed that the decision policy proposed in this work, relies on the parameters including the person power (immunity) S, the comorbidity power C, the virus power I, and the probability of the virus attack p_I. Thus, our approach differs from those based on the reproduction numbers R_0 and R_1 (see [61] and [62]). Just as it happens with the probability of an impulsive noise in model $\mathcal{A}$, the p_I in model $\mathcal{B}$ does not refer to the probability that the virus passes from an individual to another, but it refers to the probability that a person is exposed to an infective attack generated by the virus source. Thus, probability p_I should be considered the same regardless to "roam" or "lock" scenario. Some remarks on the possibility to measure of S, C, I and p_I are given in Sect. X.

A. DECISION MAKING BASED ON INTEGRATION OF INFORMATION

In order to increase the reliability of the decision process, and consequently taking decisions at lower risk, thresholds-based

detection in Fig. 13 can be integrated with the area experts opinions. For example, an expert opinion could be that a "roam" decision should be actually preferred because the "lock" would certainly lead to the ruin of many (small) businesses, and consequently to an increase of the MR for other reasons rather than Covid-19. In this sense, and other which are not considered herein, model $\mathcal{B}$ resembles model $\mathcal{A}$ (see the last paragraph in Sect. VI) where, in realistic conditions not modeled by our framework, a MCM scheme may perform better than SCM, even more than what it was anticipated.

To integrate such an auxiliary information in the model, it is necessary to resort to a so called *soft-information* i.e., to merge different pairs (x_i, r_i), of decision x_i and its reliability r_i, in an expression that maximizes the (Bayesian) posterior probability (MAP) of correct decision policy.

Assuming independent soft data $(x_1, r_1), (x_2, r_2), \cdots, \cdots (x_K, r_K)$, the MAP estimate $\hat{x}_{MAP}$ is defined as the mean of the weighted values x_k [63]

$$\hat{x}_{\text{MAP}} = \frac{\sum_{k=1}^{K} r_k x_k}{\sum_{k=1}^{K} r_k}. \tag{17}$$

Assuming Gaussian distributed information sources $x_k \in \mathcal{G}\left(\mu_k, \sigma_k^2\right)$, the source reliability, or Fisher information, can be defined as the inverse value of the variance, i.e., $r_k = 1/\sigma_k^2$ [63]. Then the reliability r_{MAP} and variance $\hat{\sigma}^2_{\text{MAP}}$ of the estimate $\hat{x}_{\text{MAP}}$ would be

$$r_{\text{MAP}} = \sum_{k=1}^{K} \frac{1}{\sigma_k^2}, \quad \text{and} \quad \hat{\sigma}^2_{\text{MAP}} = \frac{1}{\sum_{k=1}^{K} \frac{1}{\sigma_k^2}}. \tag{18}$$

Given (17), the decision policy which should minimize the MR, works as follows:

- if $\hat{x}_{\text{MAP}} \leq \gamma_T$ decide for the "roam" scenario;
- if $\hat{x}_{\text{MAP}} > \gamma_T$ decide for the "lock" scenario;

where $\gamma_T = 1/\text{SIR}_T$ is given by (16).

Here, symbols x_k represent independent (mean) estimates of the $\gamma_I = 1/\text{SIR}$. Note that when x_k represents an index (percentual) value, the MAP estimate has to be defined as the geometric mean instead of the arithmetic mean. Independent information sources are the most convenient case. For correlated sources, an expression for the MAP estimate can be found in [64].

B. MAP DECISION EXAMPLE

Let's assume the management team to be focused on a specific population, either located in a specific country or a certain region, a town, etc. Let's also assume that the team wants to take decisions not only by means of the decision policy we described for model $\mathcal{B}$, but it prefers to take a Bayesian MAP decision by using (17), which enables them to include also opinions of independent experts. An expert opinion is preferred to be expressed in an extremely simple form like, "*in my opinion I suggest "roam" with 95 % confidence*", or possibly another one "*in my opinion I suggest "lock" with 70 % confidence*", etc. Based on the experts opinion, it is easy to compute the reliability of the opinion assuming a Gaussian distribution for each test statistic.

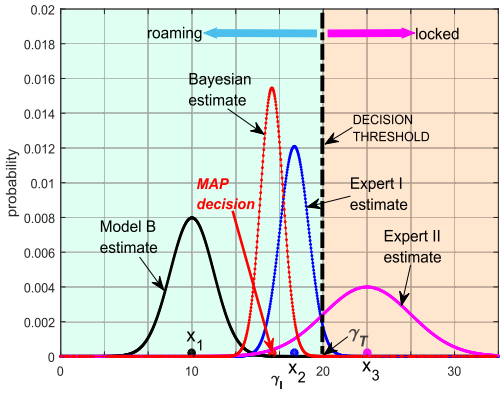

FIGURE 14. An example of the decision making based on the Bayesian integration of the model result and the two experts opinions.

Fig. 14 shows an example of exploiting a Bayesian MAP decision by using (17), where the soft data provided by model $\mathcal{B}$ is integrated with opinions provided by two independent experts. For considered estimators, including model $\mathcal{B}$, expert I and expert II, Fig. 14 shows *pdf*'s of the corresponding Gaussians *pdf*'s for estimates whose modes are x_1, x_2 and x_3, respectively.

Let's assume that the coronavirus monitoring system for the considered population provides S=1, SCR=25dB, SIR= −10dB (i.e., I=10), and $p_I = 0.001$. Thus, the decision threshold for model $\mathcal{B}$ associated with these values can be computed from (16), leading to $\gamma_T = 20$, i.e., $\text{SIR}_T = -13$dB.

Assuming the confidence (see e.g. [63]) for the model $\mathcal{B}$ estimate is ±5%, then the corresponding Gaussian *pdf* of the estimate is depicted on Fig. 14 with the mode at $\gamma_I = x_1 = 10$, (i.e., SIR=0.1). Regarding the threshold $\gamma_T = 20$ it corresponds to about 99.8% confidence for "roam", and only 0.2% for the "lock" decision. The confidence for experts opinions are obtained by the expert I with 95 % confidence, and by the expert II with 30 % confidence for "roam" scenario, which results to $\gamma_I = x_2 \approx 17$ and $\gamma_I = x_3 \approx 23$, respectively. As shown in Fig. 14, the Bayesian decision $\hat{x}_{\text{MAP}} \approx 16$ obtained by (17) results in "roam" decision with about 99.5 % confidence. Thus, although expert II suggests the "lock" decision with 70% confidence, in a contrast to $\mathcal{B}$ and expert I, Bayesian decision is "roam" with negligible risk.

X. SOME REMARKS

In model $\mathcal{A}$ the SER results depend on p_I (the probability of the impulsive event), the SIR (signal-power to impulse-noise-power ratio), as well as on the SNR (signal-power to the "white"-noise-power ratio). Equivalently, the MR results for model $\mathcal{B}$ depend on p_I (probability of the virus attack) and the SIR (person power to virus power ratio) as well as on the

SCR (person power to comorbidity power ratio). Obviously, both models are similarly structured, and all the parameters are Rayleigh distributed, since all related RVs are composed of the two mutually independent components for $\mathcal{A}$ represent the magnitude of complex-valued RV which, while for model $\mathcal{B}$ they represent the real random variables associated with physical and psychological/social conditions.

A. MORE ON THE MR PREDICTION

In order to confidently estimate the MR by the proposed model $\mathcal{B}$, it is enough to confidently estimate the model parameters p_I, SIR and SCR. Although this could be sub-optimal, we may think to separately estimate the population parameters including S and C, as well as the coronavirus parameters including the virus power I and the virus attack probability p_I, for the considered population. This could be a more efficient and reliable approach, with respect to the usual methods employed for Covid-19, which are based on tracking of the reproduction factors and the prediction of the pandemic wave. Note, however, that all the parameters that are necessary for the MR prediction, including SCR, SIR and p_I, which should be clinically and epidemiologically identified by virology and epidemiology experts. Simple methods to estimate the model $\mathcal{A}$ parameters, based on practical real field measurements can be found in [45], [65]. Similarly, guided by the assumed equivalence, real field (clinical and epidemiological) measurements have to be used to clearly define and estimate the latent parameters in model $\mathcal{B}$.

Assuming that model $\mathcal{B}$, obtained by reinterpreting the SCM/MCM model $\mathcal{A}$, can be proven by experts to be sufficiently accurate and meaningful, the results shown in sections VII. - X. may be considered as statistically predicted results of the MR. It would be obviously interesting to compare these analytical results, as well as the effectiveness of the proposed control strategy, on real life scenarios in a sufficiently long and dynamically controlled (lock/roam) period.

Based on the last observations, it should be clear that the specific results, as well as the decision/management chart for Covid-19 scenario presented in this work, should be exclusively considered as a hopefully interesting and intriguing new point of view to virologists and Covid-19 domain-experts, but should not be used in any case as an ''instruction booklet'' for any decision/management policy for Covid-19.

Finally, note that, for simplicity, in this paper we used 2-GMM impulsive noise in model $\mathcal{A}$, which we successively re-interpreted for the Covid-19 case. However, we remind that the SCM/MCM systems $\mathcal{A}$ is more effectively described by the more general K-GMM model of the impulsive noise. Similarly, for Covid-19, influenza, and its mutations, a more general K-GMM model can be used to obtain a better fit to reality. Actually, in this case each virus mutation could play the role of a single Gaussian component among $K-1$ ones. It is important to note that Gaussian mixtures or Rayleigh mixtures, expressed by K-GMM or K-RMM, can represent any nonGaussian distributions of virus variants and related parameters, either exactly or with a good approximation.

B. REMARKS ON COVID-19 HEALING AND VACCINATION

To further extend the approach presented in Sect. VII A, i.e., assuming that the models SCM/MCM and Covid-19 are conceptually equivalent, we may also think that the ImpN mitigation techniques and analysis, classically derived for communication systems, could mimic Covid-19 treatments, as well as channel coding techniques and analysis could mimic a Covid-19 vaccination campaign. As shown in [19], [24], simple mitigation techniques, based on the ImpN detection threshold (9), such as blanking, clipping or Bayesian attenuation, significantly improve the system performance, by maximizing the output signal-to-noise ratio, and consequently by minimizing the SER [4]. Besides that, channel coding [66], [67] can be implemented by introducing redundancy in the signal or symbol space, which can additionally improve the system performance in optimal or sub-optimal ways. Such codes span from multidimensional M-QAM symbols, block codes and convolutional codes, up to more sophisticated and almost optimal low density parity check (LDPC) codes [68].

Thus, any realistic communication system working in an impulsive environment, could apply only ImpN mitigation to minimize the SER [4], [20]. However, if the obtained SER is not sufficiently low, the systems might also use some kind of additional (redundant) channel coding [69]. Actually, in an impulsive environment, it is not reasonable to use only channel coding, since the coding redundancy is optimized to the AWGN channels, and consequently such a redundancy is not efficiently exploited in channel affected by ImpN [18], [70]. It is important to note that, due to the unsufficient redundancy, the decoder generates its own (internal) errors which results in even worse SER performance [66], [67].

The benefit of using ImpN mitigation in SCM/MCM systems can be briefly explained by the following:

i) the total power of the mitigated ImpN is reduced [19], [24], and the noise distribution approximates more or less a Gaussian distribution [4], which can significantly reduce the SER,
ii) since the mitigated impulsive noise can be approximately considered as a white noise, if necessary, a redundant coding can be efficiently applied to further reduce the SER.

Translating these considerations this to the Covid-19 scenario, we may conclude the following:

1) healing of ''significantly infected individuals'' noticeably reduces the spreading of an infective virus over the population, thus directly reducing the mortality rate (MR),
2) the ''healed'' population, which comprises healed ''significantly infected individuals'', can be approximately considered as a ''Covid-19-free'' population, with the MR that is relatively acceptably low. However, if necessary, vaccination (like for influenza) can be additionally applied to further reduce the MR. Note that the findings in model $\mathcal{A}$ would suggest, if such a re-interpretation is

correct, that vaccination itself, without previous treatment of (highly) infected individuals, could result in an even worse MR.

Obviously, the healing treatment, as well as the threshold (criterion) to detect those ''highly infected individuals'' that should undergo the treatment, are expected to be considered by experts.

XI. CONCLUSION

We compared SER performance of SCM and MCM communication systems affected by impulsive noise for unmitigated scenario. The results show that MCM performs better than SCM systems, when the probability and power of the impulse noise are not too high. This conclusion can be found a bit surprising since, in single carrier systems, an impulse will impact just a single symbol, whereas in MCM the impact of the impulse is spread over all the data symbols. Assuming that Covid-19 conceptually performs in a similar way, we may conclude that the ''roam'' scenario will result in a lower MR than the ''lock'' scenario, in situations when either the probability of a virus attack or the virus power are not too high. Conversely, when both the probability of the virus attack and the virus power are relatively high, the ''lock'' scenario performs better than the ''roam'' scenario. Based on these results, an adaptive optimal decision/management policy, supported by the criterion of a minimal MR, is presented. The proposed policy relies on a binary ''roam/lock'' decision test, with an optimal threshold that is set to guarantee the minimal MR.

Following the above-mentioned findings, an optimal Covid-19 control policy should not necessarily assume that the isolation of individuals (e.g., lockdown) implies a priori the minimal MR. Conversely, as it happens in the absence of a pandemic, the ''roam'' scenario (normal living) should be assumed as the one that potentially guarantees the lower MR, as long as the pandemic parameters are below a certain threshold. Then, when the threshold is violated, the control system has to switch to the ''lock'' scenario. Furthermore, the number of infected individuals should not be necessarily considered as the indicator of the virus power; it may be more safely identified by the percentage of infected people that suffer serious consequences. Actually, the prediction of the MR and the decision/management policy, should be based on the measured Covid-19 parameters, including the virus power, the probability of the virus attacks, as well as the immunity and the comorbidity power.

The last subsection in this work highlighted some aspects based on the reinterpretation of the SER results in mitigated and encoded SCM/MCM systems. These results may inspire some future work that could come-up with a more elaborated analysis of the SER and, along the line of the proposed conceptual similarity, of the MR results. Future research directions may also consider pseudoperiodic (bursty) impulsive (virus) attacks, modelled by a two-state Markov-Gaussian process, and the associated decision/management policy chart.

ACKNOWLEDGMENT

The authors are also grateful to Prof. Josko Radic for fruitful discussions during the work on the manuscript, as well as to Katarina Rados for the technical support.

REFERENCES

[1] J. Proakis, *Digital Communications*, 5th ed. New York, NY, USA: McGraw-Hill, 2008.
[2] P. Banelli and L. Rugini, ''OFDM and multicarrier signal processing,'' in *Academic Press Library in Signal Processing*, vol. 2. Amsterdam, The Netherlands: Elsevier, 2014, pp. 187–293.
[3] M. Ghosh, ''Analysis of the effect of impulse noise on multicarrier and single carrier QAM systems,'' *IEEE Trans. Commun.*, vol. 44, no. 2, pp. 145–147, Feb. 1996.
[4] N. Rožić, P. Banelli, D. Begusić, and J. Radić, ''GMM-based symbol error rate prediction for multicarrier systems with impulsive noise suppression,'' *IEEE Trans. Veh. Technol.*, pp. 1–15, 2021.
[5] R. Pastor-Satorras and A. Vespignani, ''Epidemic spreading in scale-free networks,'' *Phys. Rev. Lett.*, vol. 86, no. 14, pp. 3200–3203, Apr. 2001.
[6] I. Ciufolini and A. Paolozzi, ''Mathematical prediction of the time evolution of the COVID-19 pandemic in Italy by a Gauss error function and Monte Carlo simulations,'' *Eur. Phys. J. Plus*, vol. 135, no. 4, p. 355, Apr. 2020.
[7] L. Jiang, Q. Xu, H. Pan, Y. Da, and J. Tong, ''Virus propagation in wireless sensor networks with media access control mechanism,'' *Secur. Commun. Netw.*, vol. 2020, Nov. 2020, Art. no. 6513920.
[8] S. Goel and S. F. Bush, ''Biological models of security for virus propagation in computer networks,'' Univ. Albany, State Univ. New York, Tech. Rep., 2004, pp. 1–7. [Online]. Available: https://www.albany.edu/goel/publications/goellogin12004.pdf
[9] E. A. Hagras, ''Performance analysis of single carrier and multicarrier IDMA signals in non-Gaussian impulsive channel,'' in *Proc. 32nd Nat. Radio Sci. Conf. (NRSC)*, Mar. 2015, pp. 155–162.
[10] S. Miyamoto, M. Katayama, and N. Morinaga, ''Performance analysis of QAM systems under class A impulsive noise environment,'' *IEEE Trans. Electromagn. Compat.*, vol. 37, no. 2, pp. 260–267, May 1995.
[11] D. Middleton, ''Statistical-physical models of electromagnetic interference,'' *IEEE Trans. Electromagn. Compat.*, vol. EMC-19, no. 4, pp. 106–127, Aug. 1977.
[12] D. Middleton, ''Non-Gaussian noise models in signal processing for telecommunications: New methods an results for class A and class B noise models,'' *IEEE Trans. Inf. Theory*, vol. 45, no. 4, pp. 1129–1149, May 1999.
[13] M. Shao and C. L. Nikias, ''Signal processing with fractional lower order moments: Stable processes and their applications,'' *Proc. IEEE*, vol. 81, no. 7, pp. 986–1010, Jul. 1993.
[14] Y. H. Ma, P. L. So, and E. Gunawan, ''Performance analysis of OFDM systems for broadband power line communications under impulsive noise and multipath effects,'' *IEEE Trans. Power Del.*, vol. 20, no. 2, pp. 674–682, Apr. 2005.
[15] P. Amirshahi, S. M. Navidpour, and M. Kavehrad, ''Performance analysis of uncoded and coded OFDM broadband transmission over low voltage power-line channels with impulsive noise,'' *IEEE Trans. Power Del.*, vol. 21, no. 4, pp. 1927–1934, Oct. 2006.
[16] K. Khalil, P. Corlay, F.-X. Coudoux, M. G. Gazalet, and M. Gharbi, ''Analysis of the impact of impulsive noise parameters on ber performance of OFDM power-line communications,'' in *Proc. Int. Symp. Signal, Image, Video Commun. (ISIVC)*, 2014, pp. 1–4.
[17] J.-J. Seo, S.-J. Cho, and K. Feher, ''Impact of non-Gaussian impulsive noise on the performance of high-level QAM,'' *IEEE Trans. Electromagn. Compat.*, vol. 31, no. 2, pp. 177–180, May 1989.
[18] J. Haring and A. J. H. Vinck, ''Coding and signal space diversity for a class of fading and impulsive noise channels,'' *IEEE Trans. Inf. Theory*, vol. 50, no. 5, pp. 887–895, May 2004.
[19] S. V. Zhidkov, ''Performance analysis and optimization of OFDM receiver with blanking nonlinearity in impulsive noise environment,'' *IEEE Trans. Veh. Technol.*, vol. 55, no. 1, pp. 234–242, Jan. 2006.
[20] S. V. Zhidkov, ''Analysis and comparison of several simple impulsive noise mitigation schemes for OFDM receivers,'' *IEEE Trans. Commun.*, vol. 56, no. 1, pp. 5–9, Jan. 2008.
[21] P. Banelli and L. Rugini, ''Impulsive noise mitigation for wireless OFDM,'' in *Proc. IEEE 16th Int. Workshop Signal Process. Adv. Wireless Commun. (SPAWC)*, Stockholm, Sweden, Jun. 2015, pp. 346–350.

[22] D. Darsena, G. Gelli, F. Melito, and F. Verde, "ICI-free equalization in OFDM systems with blanking preprocessing at the receiver for impulsive noise mitigation," *IEEE Signal Process. Lett.*, vol. 22, no. 9, pp. 1321–1325, Sep. 2015.

[23] L. Rugini and P. Banelli, "On the equivalence of maximum SNR and MMSE estimation: Applications to additive non-Gaussian channels and quantized observations," *IEEE Trans. Signal Process.*, vol. 64, no. 23, pp. 6190–6199, Sep. 2016.

[24] N. Rožić, P. Banelli, D. Begusić, and J. Radić, "Multiple-threshold estimators for impulsive noise suppression in multicarrier communications," *IEEE Trans. Signal Process.*, vol. 66, no. 6, pp. 1619–1633, Mar. 2018.

[25] N. H. Nguyen, B. Berscheid, and H. H. Nguyen, "Fast-OFDM with index modulation for NB-IoT," *IEEE Commun. Lett.*, vol. 23, no. 7, pp. 1157–1160, Jul. 2019.

[26] H. S. Hussein, A. S. Mubarak, O. A. Omer, U. S. Mohamed, and M. Salah, "Sparse index OFDM modulation for IoT communications," *IEEE Access*, vol. 8, pp. 170044–170056, 2020.

[27] W. O. Kermack and A. G. McKendrick, "A contribution to the mathematical theory of epidemics," *Proc. Roy. Soc. London A, Containing Papers Math. Phys. Character*, vol. 115, pp. 700–721, Aug. 1927.

[28] T. Harko, F. S. N. Lobo, and M. K. Mak, "Exact analytical solutions of the susceptible-infected-recovered (SIR) epidemic model and of the SIR model with equal death and birth rates," 2014, *arXiv:1403.2160*.

[29] P. Bruce, "COVID-19: Epidemiological models vs. statistical models," in *Elder Research: Analytics Assessment Roadmap Brochure*. Arlington, VA, USA: Institute for Statistics Education, Statistics.Com, 2020, pp. 1–2. [Online]. Available: https://www.elderresearch.com/blog/covid-19-epidemiological-models-vs-statistical-models/

[30] F. Wong and J. J. Collins, "Evidence that coronavirus superspreading is fat-tailed," *Proc. Nat. Acad. Sci. USA*, vol. 117, no. 47, pp. 29416–29418, Nov. 2020. [Online]. Available: https://www.pnas.org/content/117/47/29416

[31] L. Zhuang and N. Cressie, "Bayesian hierarchical statistical SIRS models," *Stat. Methods Appl.*, vol. 23, no. 4, pp. 601–645, 2014.

[32] A. Rădulescu, C. Williams, and K. Cavanagh, "Management strategies in a SEIR-type model of COVID 19 community spread," *Sci. Rep.*, vol. 10, no. 1, p. 21256, Dec. 2020.

[33] M. Jamshidi, A. Lalbakhsh, J. Talla, Z. Peroutka, F. Hadjilooei, P. Lalbakhsh, M. Jamshidi, L. La Spada, M. Mirmozafari, M. Dehghani, A. Sabet, S. Roshani, S. Roshani, N. Bayat-Makou, B. Mohamadzade, Z. Malek, A. Jamshidi, S. Kiani, H. Hashemi-Dezaki, and W. Mohyuddin, "Artificial intelligence and COVID-19: Deep learning approaches for diagnosis and treatment," *IEEE Access*, vol. 8, pp. 109581–109595, 2020.

[34] R. Reiner and R. Barber, "Modeling COVID-19 scenarios for the United States," *Nature Med.*, vol. 27, pp. 94–105, Oct. 2021.

[35] G. Giordano, F. Blanchini, R. Bruno, P. Colaneri, A. Di Filippo, A. Di Matteo, and M. Colaneri, "Modelling the COVID-19 epidemic and implementation of population-wide interventions in Italy," *Nature Med.*, vol. 26, no. 6, pp. 855–860, Jun. 2020.

[36] G. Soldi, N. Forti, D. Gaglione, P. Braca, L. M. Millefiori, S. Marano, P. K. Willett, and K. R. Pattipati, "Quickest detection and forecast of pandemic outbreaks: Analysis of COVID-19 waves," *IEEE Commun. Mag.*, vol. 59, no. 9, pp. 16–22, Sep. 2021.

[37] L. Li, Z. Yang, Z. Dang, C. Meng, J. Huang, H. Meng, D. Wang, G. Chen, J. Zhang, H. Peng, and Y. Shao, "Propagation analysis and prediction of the COVID-19," *Infectious Disease Model.*, vol. 5, pp. 282–292, Mar. 2020.

[38] M. Kröger and R. Schlickeiser, "Analytical solution of the SIR-model for the temporal evolution of epidemics. part A: Time-independent reproduction factor," *J. Phys. A: Math. Theor.*, vol. 53, no. 14, p. 38, 2021.

[39] T. Ekiz, M. Kara, and L. Özçakar, "Measuring grip strength in COVID-19: A simple way to predict overall frailty/impairment," *Heart Lung*, vol. 49, no. 6, pp. 853–854, Nov. 2020.

[40] University of Washington. (2021). *COVID-19 Trends and Impact Surveys*. Elder Research: Analytics Assessment Roadmap Brochure. [Online]. Available: https://covid19.healthdata.org/united-states-of-america?view=social-distancing-tab=trend

[41] Z. Wang and G. B. Giannakis, "Wireless multicarrier communications," *IEEE Signal Process. Mag.*, vol. 17, no. 3, pp. 29–48, May 2000.

[42] S. A. Kassam, *Signal Detection Non-Gaussian Noise*, 1st ed. Philadelphia, PA, USA: Dowden & Culver, 1988.

[43] T. Y. Al-Naffouri, A. A. Quadeer, and G. Caire, "Impulse noise estimation and removal for OFDM systems," *IEEE Trans. Commun.*, vol. 62, no. 3, pp. 976–989, Mar. 2014.

[44] S. Hur, S. Baek, B. Kim, Y. Chang, A. F. Molisch, T. S. Rappaport, K. Haneda, and J. Park, "Proposal on millimeter-wave channel modeling for 5G cellular system," *IEEE J. Sel. Topics Signal Process.*, vol. 10, no. 3, pp. 454–469, Apr. 2016.

[45] K. L. Blackard, T. S. Rappaport, and C. W. Bostian, "Measurements and models of radio frequency impulsive noise for indoor wireless communications," *IEEE J. Sel. Areas Commun.*, vol. 11, no. 7, pp. 991–1001, Sep. 1993.

[46] M. G. Sanchez, L. de Haro, M. C. Ramon, A. Mansilla, C. M. Ortega, and D. Oliver, "Impulsive noise measurements and characterization in a UHF digital TV channel," *IEEE Trans. Electromagn. Compat.*, vol. 41, no. 2, pp. 124–136, May 1999.

[47] E. E. Kuruoglu, C. Molina, and W. J. Fitzgerald, "Approximation of alpha-stable probability densities using finite Gaussian mixtures," in *Proc. EUSIPCO*, Rhodes, Greece, Sep. 1998, pp. 1–4.

[48] N. Rozic, M. Russo, M. Saric, J. Radic, and D. Begusic, "Short report on approximation of the symmetric alpha-stable density by GMM," FESB, Split, Croatia, Tech. Rep. p023-02311924-060212, 2013.[Online]. Available: http://lab405.fesb.hr/sas/

[49] H. N. Hamdan and J. P. Nolan, "Estimating the parameters of infinite scale mixtures of normals," in *Proc. 36th Symp. Interface*, 2004, pp. 1–16.

[50] M. Evans, N. Hastings, and B. Peacock, *Statistical Distributions*, 3rd ed. Hoboken, NJ, USA: Wiley, 2000.

[51] T. Schonhoff and A. Giordano, *Detection and Estimation Theory and Its Applications*, 1st ed. London, U.K.: Pearson, 2006.

[52] H. B. Eriksson, P. Odling, T. Koski, and P. Borjesson, "A genie-aided detector with a probabilistic description of the side information," in *Proc. IEEE Int. Symp. Inf. Theory*, Whistler, BC, Canada, Sep. 1995, p. 332.

[53] S. Liu, K. Liu, H. Chiang, J. Zhang, and T. Chang, "Continuous learning and inference of individual probability of SARS-CoV-2 infection based on interaction data," *Sci. Rep.*, vol. 11, no. 1, pp. 2624–2633, Dec. 2021.

[54] J. Hu and N. C. Beaulieu, "Accurate simple closed-form approximations to Rayleigh sum distributions and densities," *IEEE Commun. Lett.*, vol. 9, no. 2, pp. 109–111, Feb. 2005.

[55] D. M. Drumheller and H. Lew, "Pade approximations to matched-filter amplitude probability functions- Rayleigh mixtures and multiple observations," *IEEE Trans. Aerosp. Electron. Syst.*, vol. 38, no. 2, pp. 621–632, Apr. 2002.

[56] M.-S. Alouini and A. J. Goldsmith, "A unified approach for calculating error rates of linearly modulated signals over generalized fading channels," *IEEE Trans. Commun.*, vol. 47, no. 9, pp. 1324–1334, Sep. 1999.

[57] E. Carey. (2019). *Immunodeficiency Disorders*. Healthline. [Online]. Available: https://www.healthline.com/health/immunodeficiency-disorders

[58] WHO. (2020). *Coronavirus Disease (COVID-19) Pandemic*. [Online]. Available: https://www.who.int/emergencies/diseases/novel-coronavirus-2019/

[59] (2021). *Global Research on Coronavirus Disease (COVID-19)*. [Online]. Available: https://www.who.int/emergencies/diseases/novel-coronavirus-2019/

[60] J. J. L. Jacobs, "Neutralizing antibodies mediate virus-immune pathology of COVID-19," *Med. Hypotheses*, vol. 143, Oct. 2020, Art. no. 109884. [Online]. Available: https://pubmed.ncbi.nlm.nih.gov/32512289/

[61] S. Abbott, J. Hellewell, and R. N. Thompson, "Estimating the time-varying reproduction number of SARS-CoV-2 using national and subnational case counts," *Wellcome Open Res.*, vol. 5, p. 112, Dec. 2020.

[62] L. K. Shing. (2021). *Understanding 'Effective Reproduction Number'*. HKUMed. [Online]. Available: https://www.med.hku.hk/en/covid-19/articles/R0-and-Rt

[63] R. F. Bordley, "The combination of forecasts: A Bayesian approach," *J. Oper. Res. Soc.*, vol. 33, no. 2, pp. 171–174, Feb. 1982.

[64] R. L. Winkler, "Combining probability distributions from dependent information sources," *Manage. Sci.*, vol. 27, no. 4, pp. 479–487, 1981.

[65] D. Middleton, "Procedures for determining the parameters of the first-order canonical models of class A and class B electromagnetic interference [10]," *IEEE Trans. Electromagn. Compat.*, vol. EMC-21, no. 3, pp. 190–208, Aug. 1979.

[66] S. B. Wicker, *Error Control Systems for Digital Communication and Storage*, 1st ed. Upper Saddle River, NJ, USA: Prentice-Hall, 1995.

[67] J. R. Barry, E. A. Lee, and D. G. Messerschmitt, *Digital Communication*, 3rd ed. New York, NY, USA: Amazon, 2004.

[68] T. J. Richardson and R. L. Urbanke, "Efficient encoding of low-density parity-check codes," *IEEE Trans. Inf. Theory*, vol. 47, no. 2, pp. 638–656, Feb. 2001.

[69] X. Wang, Y. Gong, and B. Lin, "SER performance of orthogonal space-time block coding over fading channels with impulsive noise," in *Proc. Int. Conf. Wireless Commun., Netw. Mobile Comput.*, Sep. 2007, pp. 45–48.
[70] N. Andreado and F. N. Pavlidou, "Mitigation of impulsive noise effect on the PLC channel with QC-LDPC codes as the outer coding scheme," *IEEE Trans. Power Del.*, vol. 25, no. 3, pp. 1440–1449, Jul. 2010.

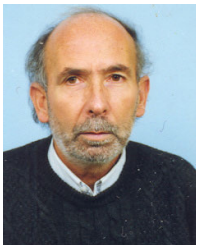

NIKOLA ROŽIĆ (Member, IEEE) received the B.S. degrees in electrical engineering and electronics from the University of Split, in 1968 and 1969, respectively, and the M.S. and Ph.D. degrees from the University of Ljubljana, Slovenia, in 1977 and 1980, respectively. Currently, he is a Professor Emeritus in electrical and computing engineering and contributes to the research team for advanced networking technologies and systems at the University of Split (FESB). His research interests include information and communication theory, signal processing, coding, and prediction methods. Since 1998, he has been serving as the TPC Co-Chair for the International Conference on Software, Telecommunications and Computer Networks (SoftCOM), which was technically co-sponsored by IEEE Communications Society (ComSoc). He is the Editorial Chair of the *Journal of Communications Software and Systems* (JCOMSS), supported by IEEE ComSoc, Technical Committee on Communications Software (TCCS). He is a member of IEEE, including ComSoc, CS, BS, APS, ITS, and SPS. Currently, he chairs the Croatian Communications and Information Society (CCIS), the sister society of the IEEE ComSoc.

PAOLO BANELLI (Senior Member, IEEE) received the Laurea degree *(cum laude)* in electronics engineering and the Ph.D. degree in telecommunications from the University of Perugia, Perugia, Italy, in 1993 and 1998, respectively. Since 2019, he has been a Full Professor with the Department of Engineering, University of Perugia, where he has been an Associate Professor, since 2005, and an Assistant Professor, since 1998. He was a Visiting Researcher with the University of Minnesota, Minneapolis, MN, USA, in 2001, and a Visiting Professor with Stony Brook University, Stony Brook, NY, USA, from 2019 to 2020. His research interests include signal processing and optimization for wireless communications, graph signal processing and learning, and signal processing for biomedical applications. He was a member of the IEEE Signal Processing for Communications and Networking Technical Committee, from 2011 to 2013. In 2009, he was the General Co-Chair of the IEEE International Symposium on Signal Processing Advances for Wireless Communications. He served as an Associate Editor for the IEEE TRANSACTIONS ON SIGNAL PROCESSING (from 2013 to 2016), *EURASIP Journal on Advances in Signal Processing* (since 2013), and IEEE OPEN JOURNAL OF SIGNAL PROCESSING (since 2020).

ANA MARUSIC is currently a Professor of anatomy and the Chair of the Department of Research in Biomedicine and Health, University of Split School of Medicine, Split, Croatia, and holds an Honorary Professorship at The University of Edinburgh, Edinburgh, U.K. She has a number of significant academic achievements including authorship of more than 300 peer-reviewed articles and was heavily involved with creating the policy of mandatory registration of clinical trials in public registries which helped change the legal regulation of clinical trials worldwide. She is also the Co-Chair of the Cochrane Scientific Committee. She is the Founder of the Cochrane Croatia and takes responsibility for research as its Research Coordinator. She is on the Steering Group, Enhancing the QUality And Transparency Of Health Research (EQUATOR) Network. She is the Co-Editor-in-Chief of the *Journal of Global Health*. She chairs the Research Committee of the World Association of Medical Editors and was the President of the European Association of Science Editors (EASE), World Association of Medical Editors (WAME), and Council of Science Editors (CSE).